Mouse BRWD1 is critical for spermatid postmeiotic transcription and female meiotic chromosome stability

Shrivatsav Pattabiraman,[1,2] Claudia Baumann,[3] Daniela Guisado,[1,2] John J. Eppig,[4] John C. Schimenti,[1,2] and Rabindranath De La Fuente[3]

[1]Department of Biomedical Sciences and [2]Center for Vertebrate Genomics, Cornell University, College of Veterinary Medicine, Ithaca, NY 14853
[3]Department of Physiology and Pharmacology, University of Georgia College of Veterinary Medicine, Athens, GA 30602
[4]The Jackson Laboratory, Bar Harbor, ME 04609

Postmeiotic gene expression is essential for development and maturation of sperm and eggs. We report that the dual bromodomain-containing protein BRWD1, which is essential for both male and female fertility, promotes haploid spermatid–specific transcription but has distinct roles in oocyte meiotic progression. Brwd1 deficiency caused down-regulation of ∼300 mostly spermatid-specific transcripts in testis, including nearly complete elimination of those encoding the protamines and transition proteins, but was not associated with global epigenetic changes in chromatin, which suggests that BRWD1 acts selectively. In females, Brwd1 ablation caused severe chromosome condensation and structural defects associated with abnormal telomere structure but only minor changes in gene expression at the germinal vesicle stage, including more than twofold overexpression of the histone methyltransferase MLL5 and LINE-1 elements transposons. Thus, loss of BRWD1 function interferes with the completion of oogenesis and spermatogenesis through sexually dimorphic mechanisms: it is essential in females for epigenetic control of meiotic chromosome stability and in males for haploid gene transcription during postmeiotic sperm differentiation.

Introduction

During spermiogenesis, round spermatids undergo complex biochemical and morphological changes as they differentiate into sperm. The spermatids elongate, acquire an acrosomal cap, and develop a tail. Most of the cytoplasm is extruded in the form of residual bodies, and the nucleus undergoes extensive condensation as the histones are replaced by protamines. This differentiation is orchestrated by a wave of gene expression that occurs exclusively after meiosis. Examples of genes transcribed postmeiotically include protamines, transition proteins, and outer dense fiber and fibrous sheath proteins of the tail. Transcription of haploid-expressed genes eventually ceases when round spermatids begin to elongate and undergo nuclear compaction (Sassone-Corsi, 2002).

One of the key proteins regulating haploid gene expression is cAMP response element modulator (CREM)-τ. CREM-τ is one of the activator isoforms of CREM that is specific to testis and is transcribed exclusively in mid-late pachytene spermatocytes and translated in round spermatids (Foulkes, 1992; Weinbauer et al., 1998). Before meiosis, a repressor isoform of CREM is expressed. Therefore, CREM-τ–activated genes are expressed exclusively after meiosis. *Crem* knockout mice are sterile and arrest at the round spermatid stage (Blendy et al. 1996; Nantel et al., 1996). Chromatin immunoprecipitation (ChIP)-Seq experiments revealed that CREM-τ binds the promoters of >6,000 genes in male germ cells, including those of the protamines, transition proteins, and other postmeiotic genes (Martianov et al., 2010). CREM-τ transcriptional activity is regulated by its coactivator activator of CREM in testis (ACT; Kotaja et al., 2004). Apart from CREM-τ, there are many testis-specific transcription factors that are either paralogues of the TFIID components (such as TAF4B and TAF7L) or are testis-specific isoforms of general transcription factors such as TATA-binding protein

Correspondence to Rabindranath De La Fuente: rfuente@uga.edu; or John C. Schimenti: jcs92@cornell.edu

Abbreviations used in this paper: ACT, activator of CREM in testis; CREM, cAMP response element modulator; GV, germinal vesicle; IAP, intracisternal A particle; MGI, Mouse Genome Informatics; SN, surrounded nucleolus; TSA, trichostatin A; WT, wild type.

The Rockefeller University Press $30.00
J. Cell Biol. Vol. 208 No. 1 53–69
www.jcb.org/cgi/doi/10.1083/jcb.201404109

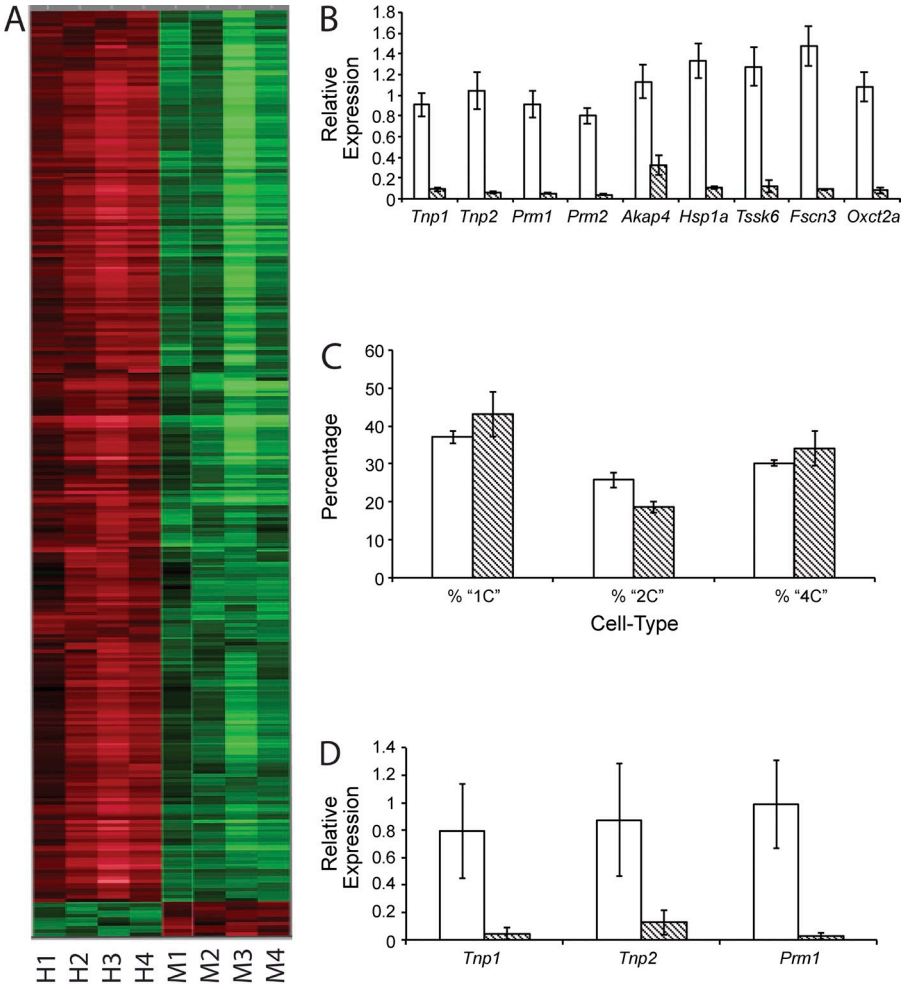

Figure 1. **Gene expression profiling of *Brwd1*$^{-/-}$ spermatids.** (A) Heat map visualization of 286 down-regulated transcripts in mutant testes from 27-d-old animals as detected by gene expression microarray analyses (H1–H4 are heterozygotes, M1–M4 are mutants). (B) Real-time PCR validation of the most down-regulated genes in 27-d-old mice. The hatched boxes represent mutant levels. (C) Flow cytometry count of testicular cells based on DNA content (C) shows that the percentage of haploid spermatids in both WT and mutant testes are the same. The 1C cells are haploid spermatids, the 2C cells correspond to somatic and spermatogonial cells that have not undergone DNA replication, and the 4C cells correspond to spermatocytes (predominantly), spermatogonia, and somatic cells that have completed S phase but not cell division. (D) Real-time PCR shows significant differences in *Tnp1*, *Tnp2*, and *Prm1* between WT and mutant transcript levels even in 21-d-old mice. Error bars indicate ±SEM. The data are the mean of three independent replicates.

(Martianov, et al., 2001). The usage of testis-specific transcriptional factors and regulators indicates that unique pathways may be used in the regulation of haploid genome expression.

Epigenetic modifications also play an important role in regulating transcription during both male and female germ cell development (De La Fuente, 2006; Sasaki and Matsui, 2008). After meiosis, histone modifications in the spermatid nucleus are necessary for transcriptional activation of the haploid genome. For instance, the promoter of the "protamine domain" containing the protamine 1 (*Prm1*), protamine 2 (*Prm2*), and transition protein 1 (*Tnp1*) genes undergoes extensive epigenetic changes as the germ cells undergo meiosis and become round spermatids. Coincident with the transcriptional activation, acetylation of histones H3 and H4 increases in the promoters and coding sequences within the protamine domain (Martins and Krawetz, 2007). H3K9 demethylation by KDM3A is also important for the transcriptional activation of the protamine domain (Okada et al., 2007). However, the mechanisms underlying epigenetic alterations specific to haploid gene expression in spermatids are not well understood, largely due to the lack of suitable in vitro model systems. Consequently, mouse models provide the most robust system for addressing the epigenetic control of gene expression in the male germline.

Functional differentiation of chromatin structure is also essential for meiotic and developmental potential of the fully grown oocyte (De La Fuente, 2006). For example, analysis of nucleoplasmin (*Npm2*$^{-/-}$) oocytes indicates that large-scale chromatin remodeling in the germinal vesicle and redistribution of major satellite sequences around the nucleolus induce the formation of a prominent heterochromatin rim or karyosphere that coincides with global transcriptional repression in preovulatory oocytes (De La Fuente et al., 2004). Although chromatin remodeling into this surrounded nucleolus (SN) configuration and global transcriptional repression are regulated through different pathways, the specialized nuclear architecture and transcriptional quiescence of the SN configuration is essential for the acquisition of both meiotic and developmental potential (De La Fuente, 2006; Abe et al., 2010).

Mice of both sexes lacking BRWD1 (bromo- and WD-containing protein-1) are infertile (Philipps et al., 2008). Sperm of mutant males exhibit aberrant morphologies including misshapen heads, a ragged mid-piece, and impaired motility. Only ∼44% of mutant oocytes developed to metaphase II when subjected to in vitro maturation, and those that reached metaphase II did not cleave to the two-cell stage after in vitro fertilization with wild-type (WT) sperm. Importantly, meiosis in males appeared completely normal, indicating that BRWD1 deficiency impacts spermiogenesis exclusively.

Whereas most infertility mutations affecting both sexes occur either in genes essential for primordial germ cells, meiosis,

or the endocrine system (Matzuk and Lamb, 2008), *Brwd1* is unique in that it appears to affect entirely different processes in sperm and oocytes (Philipps et al., 2008). BRWD1 contains two tandem bromodomains and eight WD repeats. Bromodomains are highly conserved 110–amino acid motifs that recognize acetyl-lysine residues (Hudson et al., 2000; Bottomley, 2004). This interaction is pivotal for many cellular processes, in particular chromatin remodeling and transcriptional activation (Zeng and Zhou, 2002).

Here, we provide evidence indicating that loss of BRWD1 exhibits a sexually dimorphic phenotype in male and female germ cells due to drastically different underlying mechanisms. Our results demonstrate that *Brwd1* is essential for haploid gene expression during postmeiotic germ cell differentiation during spermiogenesis. In contrast, loss of BRWD1 in preovulatory oocytes interferes with proper chromosome condensation and segregation during meiosis, resulting in severe chromosome instability associated with deregulated transposon expression and overexpression of the histone methyl transferase MLL5. Our results indicate that BRWD1 is essential for the epigenetic control of chromosome structure during female meiosis while playing a critical role in the control of haploid gene transcription during the postmeiotic differentiation events of spermiogenesis.

Results

Haploid genome transcription is disrupted in BRWD1-deficient testes

Because BRWD1 contains bromodomains typically associated with acetylated histones (Huang et al., 2003), we hypothesized that BRWD1 is involved in chromatin remodeling required for proper transcription in postmeiotic spermatids and maturing oocytes. To test this hypothesis, we performed microarray-based gene expression profiling of WT ($n = 4$) and mutant ($n = 4$) 27-d-old testes. At this stage, the first wave of germ cells has progressed to the elongating spermatid stage. In the mutant, 286 transcripts were decreased by at least twofold compared with WT, whereas 11 transcripts were overexpressed (Fig. 1 A). Expression of nine of the most down-regulated genes was tested by quantitative real-time RT-PCR (qRT-PCR), validating their underexpression (Fig. 1 B). Transcript levels of most of the underexpressed genes were decreased more than fourfold; some of them, including those corresponding to the protamines and transition protein genes, were decreased as much as 30-fold. In contrast, none of 11 potentially overexpressed genes were shown to be significant increased by real-time PCR.

To exclude the possibility that the apparent reduction in transcript levels in mutants might be caused by a delay in meiotic progression or fewer elongated spermatids in *Brwd1*$^{-/-}$ testes, two experiments were performed. First, we isolated germ cells from both WT and mutant testes, and analyzed their DNA content by flow cytometry. This quantified the relative proportions of haploid spermatids (1C content), diploid spermatogonia (most of the 2C cells), and spermatocytes (most of the 4C cells). In 27-d-old testes, there was no significant difference in the proportion of haploid cells between WT and the mutant (Fig. 1 C). Second, selected transcripts in 21-d-old WT and mutants testes

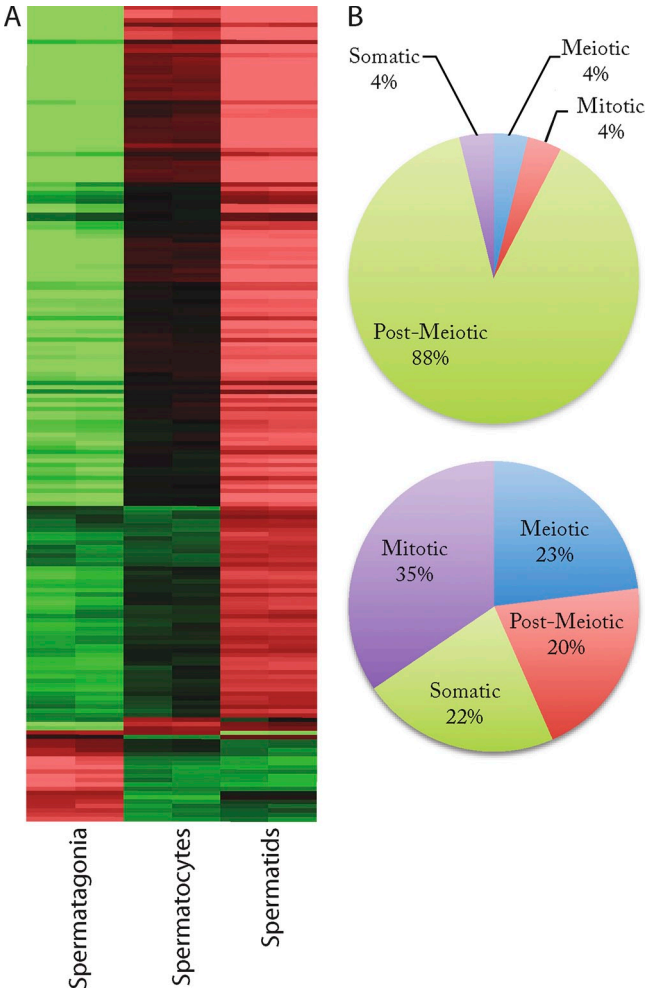

Figure 2. **Characterization of the differentially regulated genes in BRWD1-deficient testes.** (A) The heat map shows that most of the genes down-regulated in the microarray are highly expressed in spermatids. A small percentage of genes are highly expressed in spermatogonia that correlated with the up-regulated genes in the microarray. (B, top) A GermOnline-based classification of the microarray genes shows that 88% of the genes are exclusively postmeiotic. (B, bottom) Only 22% of randomly sampled germline genes are exclusively postmeiotic when similarly classified by the GermOnline database.

were compared by qPCR analyses (primarily *Prm1*, *Tnp1*, and *Tnp2*, all of which show extensive down-regulation in the microarray). Significant differences in expression were apparent at this time point, which is when haploid round spermatids first appear (Fig. 1 D). These data support the conclusion that BRWD1 is required for proper expression of postmeiotically expressed ("haploid") genes.

To test whether BRWD1 is required specifically for haploid gene expression, we classified the misexpressed genes as being meiotic, postmeiotic, or somatic using data from a comprehensive characterization of mouse spermatogenic gene expression datasets (Gattiker, et al., 2007). 46% of the genes were classified as postmeiotic, with another 48% classified as "unknown" (Fig. 2 B). Because only 5% of all known male germ cell–specific transcripts in the database are expected to be exclusively postmeiotic, our data indicate that postmeiotic genes are the predominantly affected gene class in our mutants. As

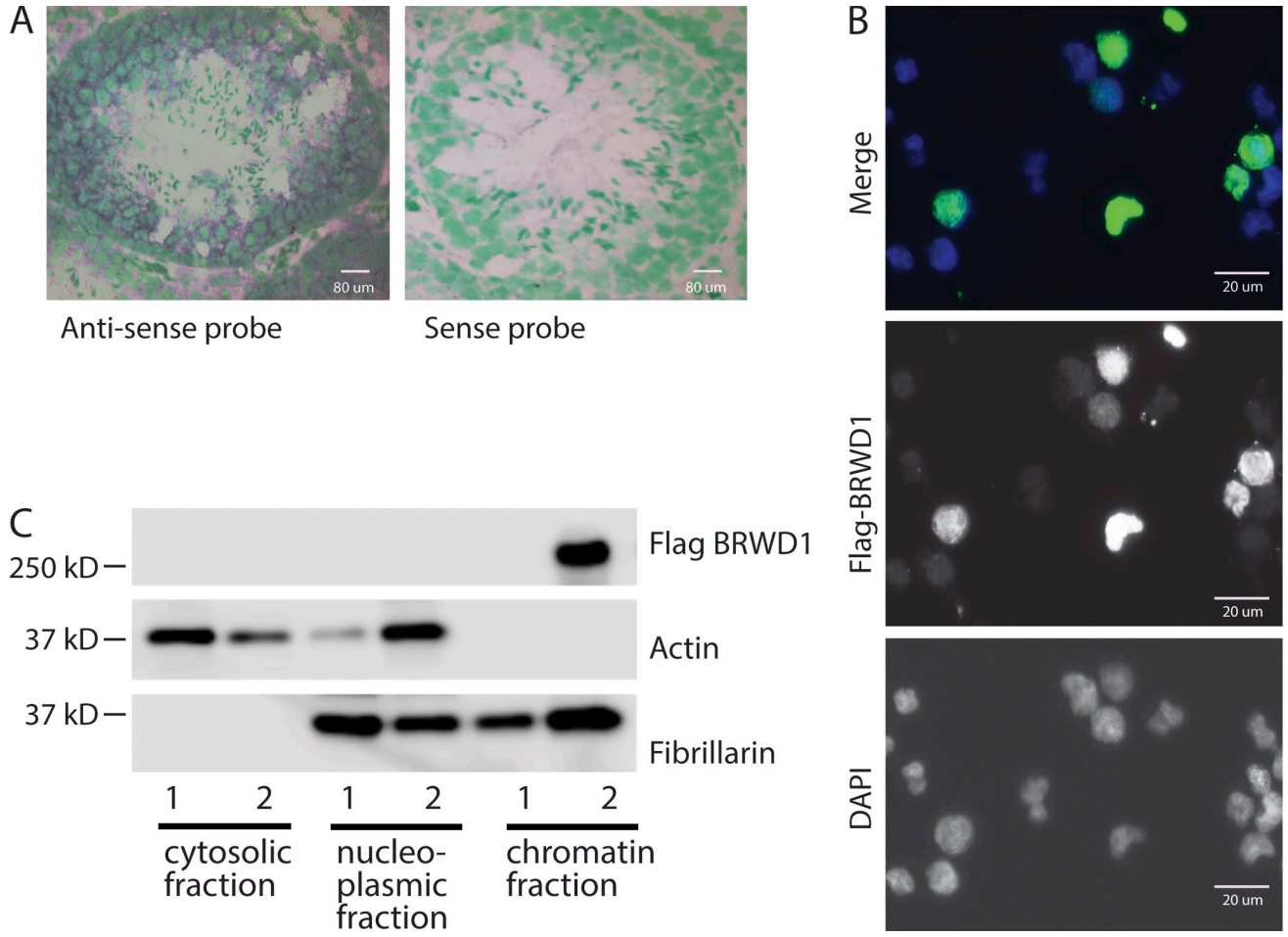

Figure 3. **BRWD1 expression and subcellular localization.** (A) RNA in situ hybridization shows robust expression of *Brwd1* in spermatocytes (Sc) and spermatids (Std; seen in blue). Nuclei are stained green using methyl-green. (B) Staining of a full-length BRWD1 expression construct tagged with an N-terminal FLAG tag in HEK cells shows predominantly nuclear localization. (C) Subcellular fractionation of HEK cells expressing FLAG-BRWD1 shows that BRWD1 was almost exclusively chromatin bound, with no protein detected in either the nucleoplasm or cytoplasm.

depicted in the heat map of the expression data in Fig. 2, almost all underexpressed genes from our experiment show high expression in the postmeiotic spermatids, and almost no expression in spermatogonia. Transcripts of some of the affected genes are present in spermatocytes, but most are exclusively postmeiotic. This suggests that BRWD1 is important for expression of postmeiotic genes during male germ cell differentiation.

Expression of BRWD1 and subcellular localization

EST data demonstrate that *Brwd1* is transcribed in a variety of tissues and cell types, including brain, testis, ovary, embryonic, and extraembryonic tissues. To identify the exact cell types expressing *Brwd1* in the testes, we performed an RNA in situ hybridization. *Brwd1* transcripts were most abundant in spermatocytes and round spermatids (Fig. 3 A).

Attempts to produce specific antibodies for the purpose of localizing BRWD1 intracellularly failed, so we expressed full-length BRWD1 bearing an N-terminal FLAG epitope in HEK cells. Clear nuclear localization was observed by immunocytology (Fig. 3 B), and Western blotting confirmed that Flag-BRWD1 localized exclusively to the nuclear, but not cytoplasmic, fraction of protein extracts (Fig. 3 C). Furthermore, BRWD1 accumulated only in the chromatin-bound, not the nucleoplasmic, protein fraction of transfected cells (Fig. 3 C), which is consistent with what would be expected of bromodomain-containing proteins.

BRWD1 deficiency does not cause gross disruption of the spermatid epigenetic landscape or pericentric heterochromatin

Epigenetic histone modifications are central to transcriptional regulation, and the process of spermatogenesis occurs in the context of dramatic and wholesale chromatin remodeling. In spermatids, a structure known as the chromocenter, containing all pericentric heterochromatin, forms in the nucleus, and its structural integrity is important for proper differentiation into sperm (Hoyer-Fender et al., 2000; Martianov et al., 2001; Kim et al., 2007). This structure appears fragmented in mice harboring a mutation in either the dual-bromodomain containing gene *Brdt* or the spermatid-specific transcription factor *Tlf*. Spermatid elongation and differentiation are compromised in these mutants (Martianov et al., 2001; Zhang et al., 2001; Shang et al., 2007; Berkovits and Wolgemuth, 2013). Because *Brwd1* ablation

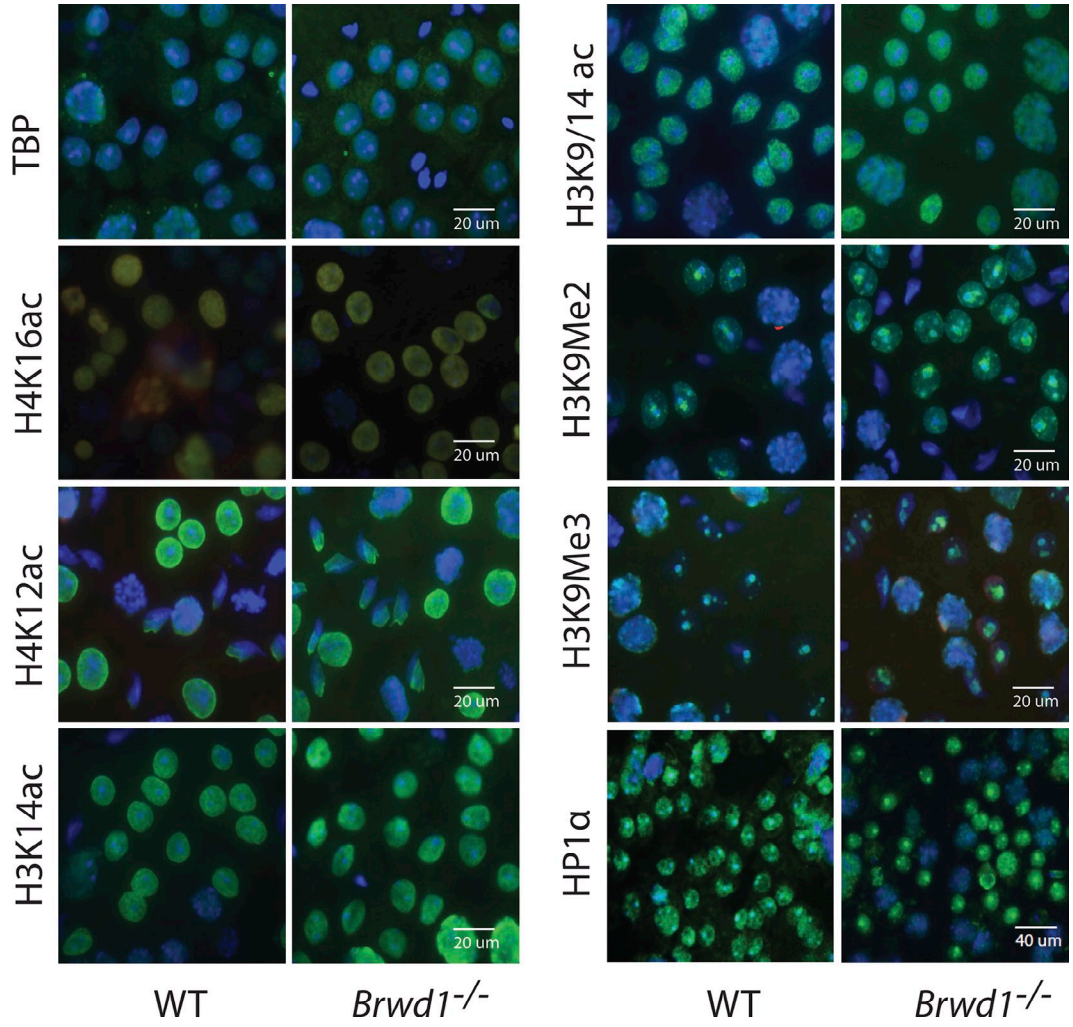

Figure 4. **Comparison of global chromatin architecture between WT and mutant spermatids.** No differences were detected in the nuclear domains marked by different epigenetic marks of histone methylation and acetylation. Chromocenter formation is also unaffected in the mutant spermatids as seen by a mostly singular focal staining of HP1. Transcription factor TBP distribution is unaffected in mutant spermatids.

disrupts gene expression and causes spermatid abnormalities resembling those in *Brdt* mutants, we hypothesized that the *Brwd1* mutant phenotype might also have a defective chromocenter. However, immunostaining of *Brwd1*$^{-/-}$ spermatids with the chromocenter marker Heterochromatin Protein 1 α (HP1α) revealed a single, nonfragmented chromocenter in all mutant spermatids, similar to WT spermatids (Fig. 4).

Apart from the clearly identifiable chromocenter, different nuclear domains are also thought to exist within the round spermatid nucleus that can be distinguished by unique epigenetic markers. For example, staining for H3K9Me2 and H3K9Me3, associated with transcriptional down-regulation, reveals unique punctate foci in the round spermatid nucleus (Liu et al., 2010). Transcription factors such as TBP and TLF also have unique distribution patterns in round spermatids (Martianov et al., 2002), and their disruption could cause transcriptional misregulation. The timely formation and maintenance of these nuclear domains is important for expression of spermatid-specific genes. We therefore hypothesized that the large-scale disruption of haploid genome expression in the *Brwd1* mutants might be caused by global defects in chromatin architecture that affect the proper formation and/or maintenance of these unique epigenetic nuclear domains. However, we detected no major differences in the distribution of the transcriptionally active epigenetic markers H4K16Ac, H4K12Ac, H3K14ac, and H3K9/14Ac, or the transcriptionally repressive epigenetic markers H3K9Me2 and H3K9Me3 between *Brwd1*$^{-/-}$ and WT spermatids (Fig. 4). Additionally, no differences were found in the distribution or intensity of transcription factor TBP staining (Fig. 4). In conclusion, the extensive misexpression of spermatid-specific genes observed in the mutants does not appear to be the result of large-scale defects in the global epigenetic landscape or chromatin structure in the mutants.

Brwd1$^{-/-}$ preovulatory oocytes have a normal protein-coding transcriptome but are defective in global transcriptional silencing

Previous studies demonstrated that oocytes from *Brwd1* mutant females have a reduced ability to complete meiotic maturation and reach the metaphase II stage after in vitro maturation (Philipps et al., 2008); however, the mechanisms involved remained to be determined. Because *Brwd1*$^{-/-}$ spermatids showed

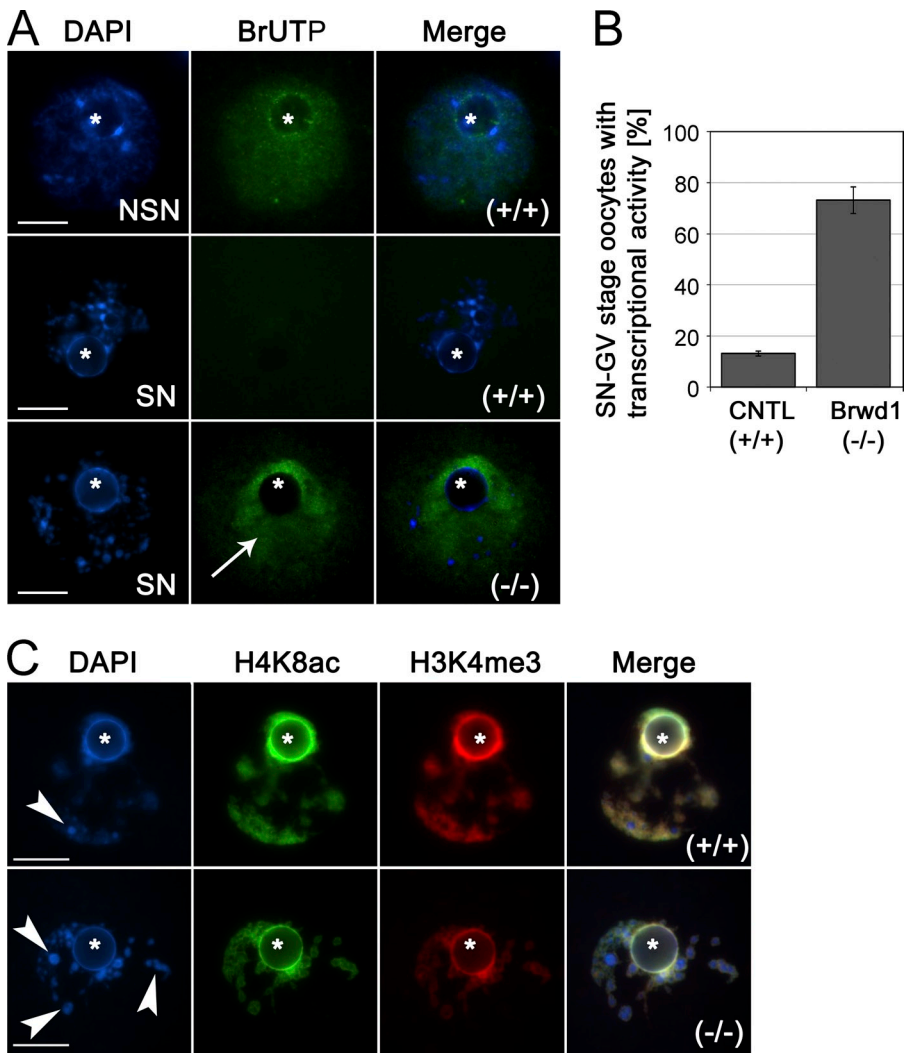

Figure 5. **Lack of global transcriptional silencing in *Brwd1* mutant oocytes.** (A) Transcription run-on assays in the germinal vesicle of preovulatory oocytes. WT oocytes (+/+) that exhibit a decondensed, nonsurrounded nucleolus (NSN) chromatin configuration incorporate high levels of bromo-UTP (BrUTP; green) into nascent RNA transcripts, resulting in diffuse nuclear staining. WT oocytes advancing to the SN configuration undergo global transcriptional silencing. *Brwd1*$^{-/-}$ oocytes fail to repress global transcriptional activity in spite of the acquisition of an SN configuration, resulting in abnormal Br-UTP incorporation throughout the nucleoplasm (arrow). The position of the nucleolus is indicated by the asterisks. (B) The proportion of WT and *Brwd1*$^{-/-}$ oocytes that exhibit persistent transcriptional activity after transition into the SN configuration. Data are presented as the mean of three independent experimental replicates ± SD (error bars). (C) Displacement of heterochromatin domains in mutant oocytes. Pericentric heterochromatin becomes associated with the nucleolus during the transition to the SN configuration in WT oocytes. Mutant oocytes exhibit histone acetylation and histone methylation marks that are indistinguishable from WT oocytes. *Brwd1*$^{-/-}$ oocytes exhibit an SN configuration; however, several pericentric heterochromatin domains fail to associate with the nucleolus (arrowheads), resulting in the formation of abnormal DAPI-stained heterochromatin clusters. Bars, 10 µm.

a dramatic disruption of spermatid-specific gene expression, we hypothesized that BRWD1 may be regulating gene expression in the female germline as well. To test this, we isolated germinal vesicle (GV) stage oocytes from both WT and mutant animals and undertook a microarray-based study. Any transcript that showed a difference of greater than twofold with a p-value <0.05 was scored as significant (Tables S2 and S3). Surprisingly, only one gene besides *Brwd1* (*Aamdc*) showed lower expression, and two genes (*Hmox1* and *Gm1564*) had higher expression in mutant oocytes. The differences from WT were only approximately twofold. These results indicate that *Brwd1* does not substantially regulate protein-coding gene transcription in the mammalian oocyte at the GV stage.

We next considered the possibility that BRWD1 is involved in regulating the transcription of noncoding RNAs. Therefore, the onset of transcriptional silencing and genome-wide histone modifications in WT and *Brwd1* mutant oocytes was compared. Transcription run-on assays after Br-UTP incorporation revealed the presence of global transcriptional activity and nascent RNA transcripts throughout the nucleoplasm in WT oocytes that exhibit a decondensed nonsurrounded nucleolus (NSN) configuration (Fig. 5 A). As expected, WT oocytes that acquire an SN configuration exhibit a global repression of nascent RNA transcripts in preparation for meiotic onset. Surprisingly, 73.5% of *Brwd1* mutant oocytes failed to repress global transcriptional activity in spite of acquiring an SN configuration (Fig. 5, A and B), and also despite a lack of evidence for increased levels of protein-coding transcripts in the microarray study.

To determine whether lack of transcriptional silencing in mutant oocytes may be caused by abnormal histone modifications, the patterns of histone acetylation and histone methylation marks associated with the establishment of a transcriptionally permissive chromatin status were compared in WT and mutant oocytes at the germinal vesicle stage. WT oocytes exhibited a prominent heterochromatin rim characteristic of the surrounded nucleolus configuration and presented only one or two DAPI-stained heterochromatin domains in the nucleoplasm that are not associated with the nucleolus (Fig. 5 C, arrowheads). Chromatin in the germinal vesicle of WT oocytes exhibited bright signals for histone H4 acetylated at lysine 8 (H4K8ac) and histone H3 trimethylated at lysine 4 (H3K4me3). No differences were observed in the establishment of H4K8ac or H3K4me3 in mutant oocytes that exhibit a distinct surrounded nucleolus configuration. However, loss of BRWD1 function increased the number of heterochromatin domains that failed to establish

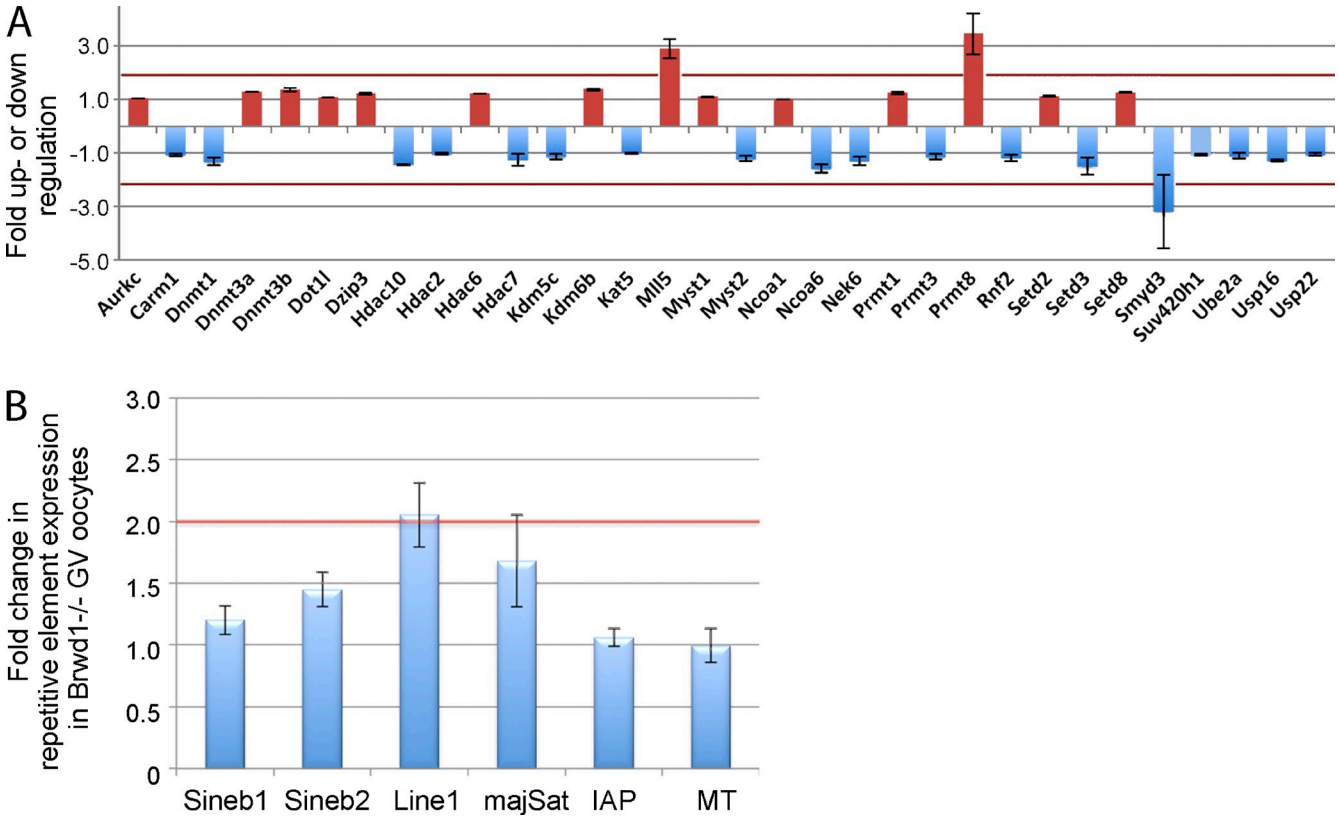

Figure 6. **Global epigenetic profiling of *Brwd1*$^{-/-}$ oocytes at the germinal vesicle stage.** (A) Overexpression of mixed lineage leukemia (MLL5) in mutant oocytes. Analysis of chromatin-modifying enzymes revealed a significant 2.89-fold overexpression of the histone H3 methyl transferase MLL5 in *Brwd1*$^{-/-}$ oocytes compared with WT oocytes. Enzymes that showed a significant change in transcript levels less than the twofold threshold (red line) are indicated. (B) *Brwd1*$^{-/-}$ oocytes exhibit a significant twofold overexpression in the levels of LINE-1 elements at the germinal vesicle stage. Data are presented as the mean ± SD (error bars) of three independent experimental replicates.

a close association with the nucleolus (Fig. 5 C, arrowheads). These results, together with the microarray study, indicate that mutant oocytes fail to repress global transcriptional activity of noncoding RNAs in preparation for the onset of meiosis and that loss of BRWD1 function affects proper chromatin condensation in the germinal vesicle of preovulatory oocytes.

Overexpression of Mixed Lineage Leukemia (MLL5) and long interspersed nuclear elements (LINES) in *Brwd1*$^{-/-}$ oocytes

The incongruence between the microarray data and the in situ run-on assay prompted us to explore technical and biological explanations. Although the microarray analysis revealed only three misregulated transcripts, it is possible that key genes involved in chromatin epigenetic modification might be misregulated to a degree not detected as significant. Therefore, a pathway-focused transcriptional profiling assay was conducted to compare the patterns of expression of key chromatin-modifying enzymes in WT and mutant oocytes at the germinal vesicle stage (Fig. 6 A). Quantitative transcriptional profiling using real-time PCR revealed a significant 2.89-fold overexpression ($P = 0.035$) of the histone methyltransferase enzyme *Mll5* in mutant oocytes. Global epigenetic profiling revealed an up-regulation of 12 chromatin-modifying enzymes and a down-regulation of 17 enzymes of less than the twofold threshold (Fig. 6 A). Loss of BRWD1 function resulted in a trend, albeit not significant ($P = 0.086$), for a 3.44-fold overexpression of the arginine methyltransferase *Prmt8* compared with WT oocytes. Notably, mutant oocytes also exhibited a 3.19-fold decrease in transcripts encoding the histone methyltransferase SMYD3, although these levels did not reach statistical significance ($P = 0.093$).

Because the real-time PCR revealed only a subtle misregulation of the chromatin-modifying genes, and more were down-regulated than up-regulated, this alone cannot explain the dramatic persistence of run-on transcription. Importantly, repetitive element probes did not exist on the gene expression microarray platform used in this study, leaving open the possibility that the continued run-on expression observed in mutant oocytes might be attributable to repetitive elements transcription. Therefore, the levels of expression of major satellite transcripts at pericentric heterochromatin, long terminal repeat (LTR) transposons such as intracisternal A particle (IAP) elements and mouse transposons (MTs) were compared, as well as nonlong terminal repeats such as SINES and LINE-1 elements (Fig. 6 B). Notably, real-time PCR analysis of preovulatory oocytes at the GV stage revealed a twofold overexpression ($P = 0.00584$) of LINE-1 elements in mutant oocytes. Combined, our results indicate that loss of BRWD1 function in preovulatory oocytes affects large-scale chromatin structure and is associated with

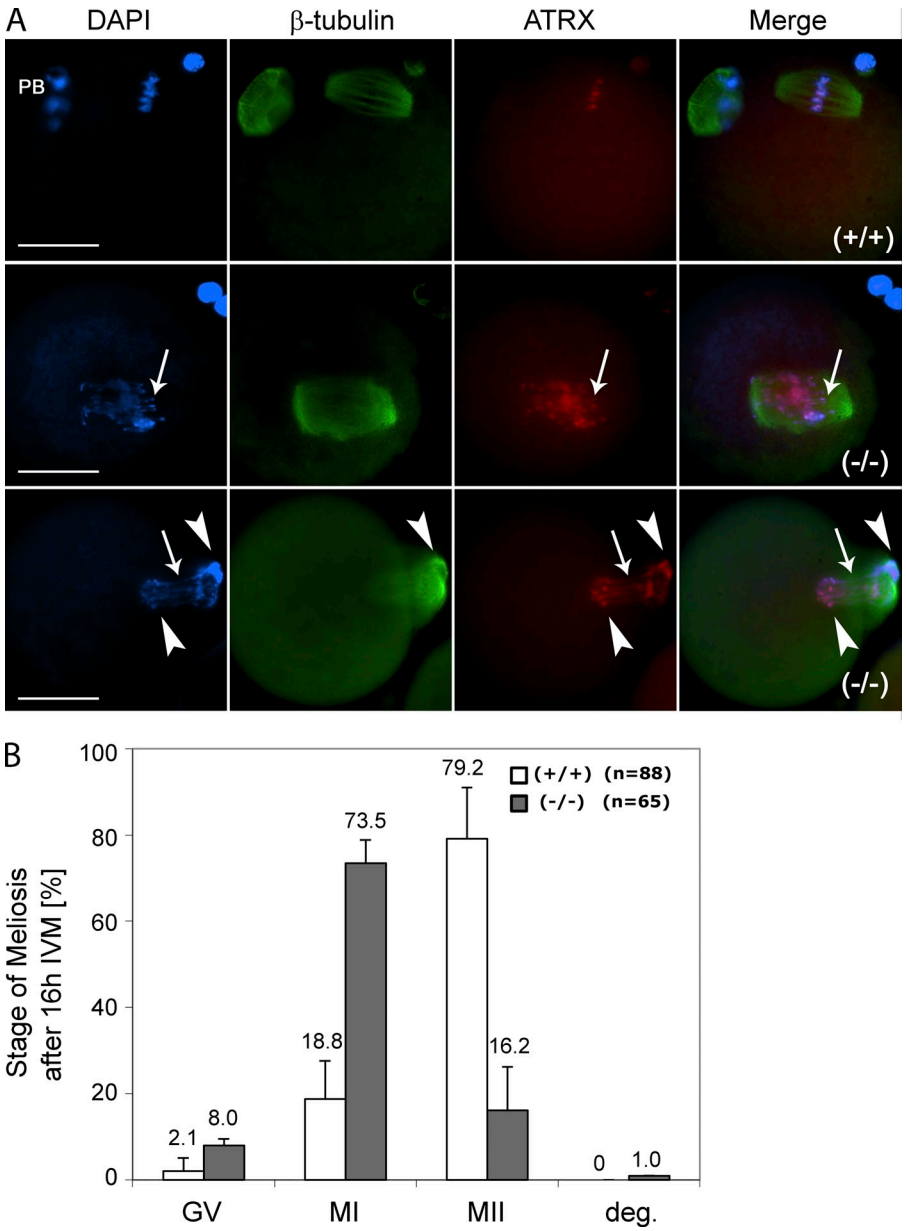

Figure 7. **Abnormal meiosis in *Brwd1*$^{-/-}$ oocytes.** (A) Meiotic progression in WT and mutant oocytes. Control oocytes progress to the metaphase II stage with chromosomes tightly aligned at a bipolar spindle. ATRX exhibits a specific pericentric heterochromatin localization. *Brwd1*$^{-/-}$ oocytes exhibit abnormal meiotic figures with elongated chromosomes (arrow) and abnormal metaphase I spindle formation. Abnormal homologous chromosome separation (arrowheads) leads to the formation of anaphase bridges (arrow) and extreme chromosome elongation. PB, polar body. Bars, 50 µm. (B) A high proportion of mutant oocytes ($P < 0.05$) arrest at metaphase I after in vitro maturation. Data are presented as mean ± SD (error bars) of four independent experimental replicates.

deregulation of two prominent epigenetic mechanisms: transposon expression and overexpression of the histone H3 lysine methyltransferase Mll5 at the germinal vesicle stage.

Loss of BRWD1 induces abnormal meiotic spindle formation, chromosome congression, and segregation defects

Developmental control of transposon expression and major satellite transcripts has recently emerged as a critical mechanism essential for chromosome stability in the female germline (De La Fuente et al., 2006; Probst et al., 2010; Su et al., 2012a,b; Fadloun et al., 2013). Therefore, a detailed analysis of large-scale chromosome structure in mutant oocytes was conducted. Analysis of meiotic configuration in WT oocytes revealed the presence of a barrel-shaped bipolar spindle with chromosomes tightly aligned at the equatorial region at metaphase II. At this stage, chromosomes also exhibit prominent staining with the chromatin-remodeling protein ATRX at pericentric heterochromatin (Fig. 7 A). In contrast, a high proportion of mutant oocytes (73.5%) exhibited metaphase I arrest due to the presence of abnormal chromosome–microtubule interactions (Fig. 7, A and B). Defects in chromosome congression cause meiotic spindle disorganization. Chromosomes in mutant oocytes exhibited ATRX staining at pericentric heterochromatin (Fig. 7 A, arrows). However, lack of proper axial chromatid condensation revealed the presence of basal ATRX staining at interstitial regions of elongated chromosomes (Fig. 7 A, middle). Lack of proper chromosome condensation also resulted in severe segregation defects with abnormal homologous chromosome separation at anaphase I, inducing severe chromatid elongation and lack of extrusion of the first polar body (Fig. 7 A, bottom).

High-resolution analysis of meiotic chromosomes revealed severe chromosome condensation and segregation defects in mutant oocytes. For example, the majority of WT oocytes

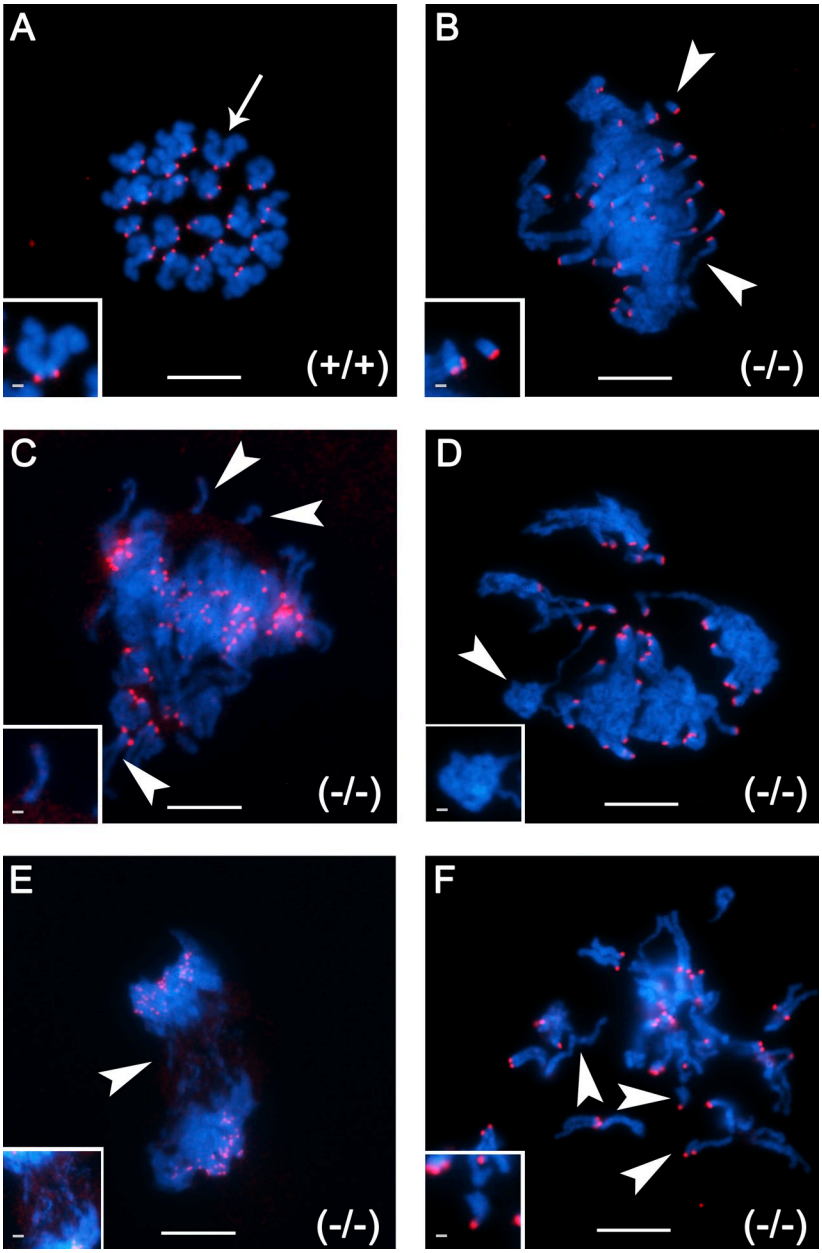

Figure 8. ***Brwd1*$^{-/-}$ oocytes exhibit chromosome instability.** (A) WT (+/+) oocyte showing a euploid chromosome complement (20 chromosomes) at the metaphase II stage. The centromere–kinetochore domains are stained with CREST (red). (B) Chromosomes from a *Brwd1*$^{-/-}$ oocyte arrested at the metaphase I stage. Note the presence of univalents (arrowheads) as well as multiple chromosome fragments (inset). (C and D) Spectrum of chromosome defects in mutant oocytes arrested at the metaphase I stage, including extreme chromosome elongation and loss of structural integrity (insets). (E) Abnormal homologous chromosome separation and anaphase bridge formation (inset). (F) Chromosome breaks in mutant oocytes at the metaphase II stage (inset). Bars: (main panels) 10 µm; (insets) 1 µm. The image in D is shown again in Fig. 9 C with additional labeling for H4K16ac.

progressed to the metaphase II stage and exhibited 20 properly condensed chromosomes (Fig. 8 A). However, at the metaphase I stage, mutant oocytes exhibited highly elongated chromosomes that were frequently found as univalents as determined by the number of CREST signals (Fig. 8 B). Moreover, meiotic spreads contained both chromatid and chromosome breaks (Fig. 8 B, arrowheads). In extreme cases, metaphase I–arrested chromosomes exhibited elongated univalent chromosomes with loss of structural integrity and multiple fragments (Fig. 8 C, arrowheads). Chromosomes in mutant oocytes exhibited CREST staining, which suggests that centromeric domains retained some kinetochore structural components. However, the extreme elongation of chromatid interstitial regions induced loss of structural integrity and formation of chromatin clusters (Fig. 8 D, arrowhead). Mutant oocytes that progressed to the metaphase II stage exhibited evidence of anaphase bridge formation with physical stretching of the chromosomes that induce multiple chromosome breaks (Fig. 8, E and F). These results indicate that loss of BRWD1 function induces severe meiotic abnormalities due to an extreme chromosome elongation phenotype. Thus, abnormal chromosome condensation in mutant oocytes interferes with proper bivalent formation, resulting in severe segregation defects and widespread chromosome instability.

Chromosomes from *Brwd1* mutant oocytes exhibit normal histone deacetylation in spite of the presence of an extreme elongation phenotype

During meiotic onset, a physiological wave of global histone deacetylation removes acetylated histone markers from condensing chromosomes in a process required for proper alignment

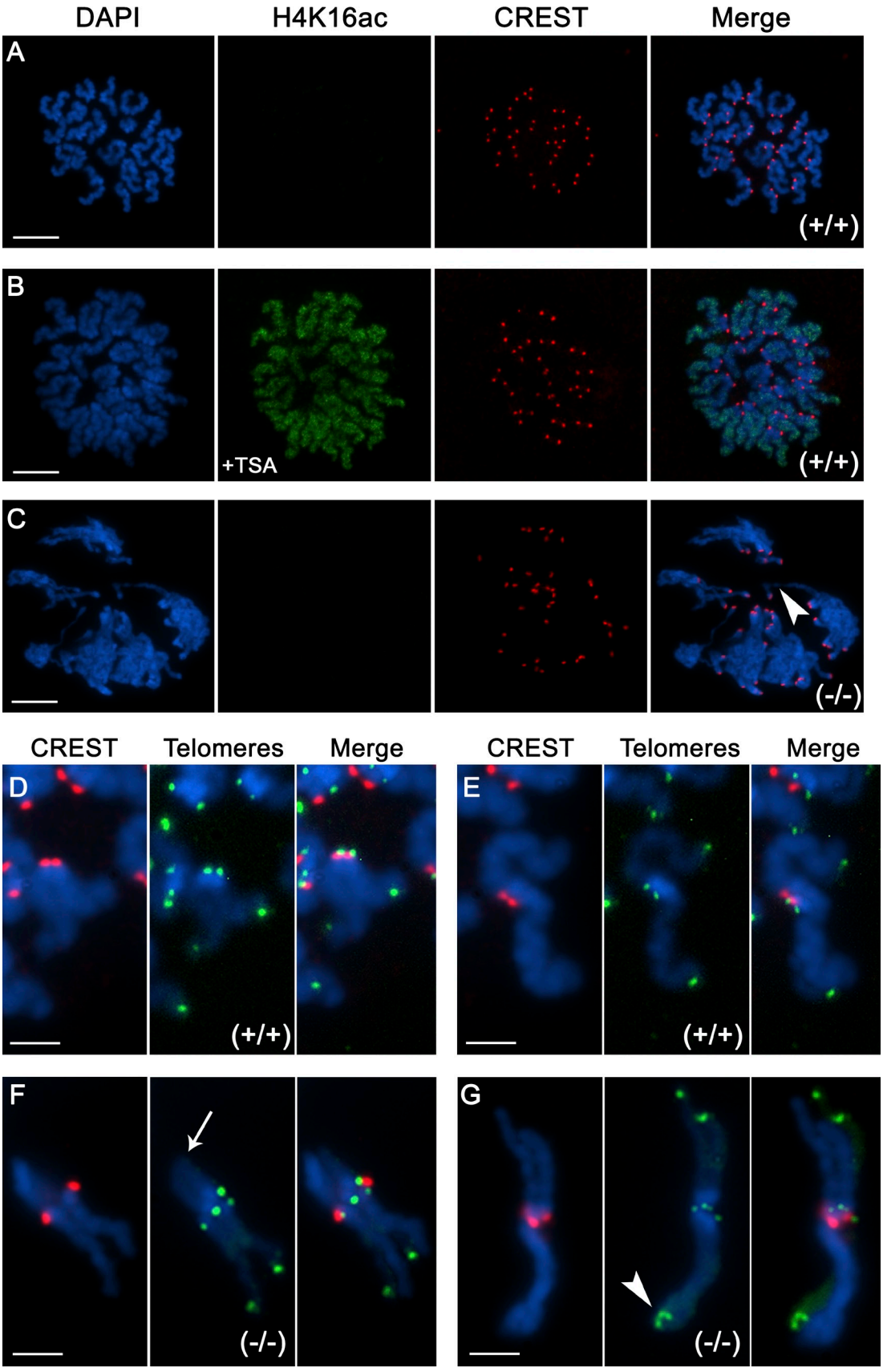

Figure 9. **Chromosomes from *Brwd1*$^{-/-}$ oocytes exhibit normal histone deacetylation but abnormal telomere structure during meiosis.** (A) WT oocytes undergo global histone deacetylation during meiosis. Note the lack of staining with histone H4 acetylated at lysine 16 (H4K16ac) on meiotic chromosomes. (B) Exposure to the histone deacetylase inhibitor TSA induces a state of genome-wide histone hyperacetylation (green) and chromatid elongation. (C) Chromosomes

and segregation in mouse oocytes (De La Fuente et al., 2004; Akiyama et al., 2006). Abnormal histone hyperacetylation during meiosis interferes with large-scale chromatin condensation and induces axial chromatid elongation in maturing mouse oocytes (Yang et al., 2012a). Therefore, we interrogated whether the chromatid elongation phenotype in mutant oocytes is caused by altered histone acetylation. WT oocytes at the metaphase II stage exhibited chromosomes that lacked histone H4 acetylated at lysine 16 (H4K16ac), which is consistent with proper global deacetylation during meiosis onset (Fig. 9 A). In accordance with previous studies (Yang et al., 2012a), exposure to the histone deacetylase inhibitor trichostatin A (TSA) induced histone hyperacetylation, resulting in bright H4K16ac staining as well as chromatid elongation (Fig. 9 B). Surprisingly, chromosomes from BRWD1-deficient oocytes exhibited normal histone deacetylation despite the presence of highly elongated chromosomes (Fig. 9 C).

Establishment and maintenance of monomethylation of histone H4 at lysine 20 (H4K20me1) is essential for proper chromosome condensation and genome integrity in mouse cells and preimplantation embryos (Oda et al., 2009; Beck et al., 2012). Therefore, we tested whether the abnormal chromosome condensation phenotype observed in mutant oocytes might be caused by abnormal levels of this critical epigenetic marker during meiosis. Notably, the majority of mutant oocytes exhibited chromosomes with H4K20me1 staining (Fig. S1). These results indicate that chromosomes from *Brwd1* mutant oocytes exhibit proper global histone deacetylation and monomethylation of histone H4 (H4K20me1), two important pathways required for chromosome stability.

Loss of axial chromatid condensation and telomere defects in *Brwd1* mutant oocytes

Previous studies using *Xenopus laevis* egg extracts indicate that condensin proteins regulate the axial shortening of metaphase chromosomes (Shintomi and Hirano, 2011). Therefore, the patterns of expression and chromosomal localization of SMC4, a condensin complex subunit required for mouse meiosis (Lee et al., 2011), were compared. Control oocytes exhibited SMC4 staining throughout the central chromatid axis of meiotic chromosomes (Fig. S2 A). Notably, SMC4 was detected in elongated chromatids in the majority of mutant oocytes, except at metaphase plates where chromosome breaks and loss of structural integrity were observed (Fig. S2 C).

Quantitative chromatin compaction assays and live cell imaging have demonstrated that axial shortening of chromatid arms begins at telomere regions and extends into the centromeric domains of a chromosome (Mora-Bermúdez et al., 2007). To determine whether abnormal axial chromatid condensation in *Brwd1*$^{-/-}$ oocytes was associated with disruption of proximal or distal telomeres, we used immuno-FISH for the simultaneous detection of the kinetochore-binding protein CREST and a DNA probe against telomeric repeat sequences. As expected, meiotic chromosomes from WT oocytes exhibited one proximal telomeric signal colocalized with CREST as well as one distal telomeric signal on each chromatid (Fig. 9, D–E). In contrast, chromosomes from mutant oocytes exhibited large distal telomeric signals forming telomere–centromere chromosome fusions (Fig. 9 F) as well as distal telomere doublets (Fig. 9 G, arrowhead). These results indicate that although the condensin protein SMC4 is present at the axial core of meiotic chromosomes in *Brwd1* mutant oocytes, loss of axial chromatid condensation is associated with abnormal distal telomere structure.

Discussion

Several genes are required for both male and female gametogenesis, but these are typically involved in common processes such as primordial germ cell development or meiosis. *Brwd1* is enigmatic in that although it is needed by both sexes for fertility, its ablation causes distinct gender-specific consequences upon gametogenesis; in males, meiotic division remains unaffected but spermiogenesis is abnormal, whereas in females, the oocyte-to-embryo transition is blocked (Philipps et al., 2008). This sexual dimorphism confounded a unifying hypothesis about the function of BRWD1 in the mammalian germline. Based on known roles of bromodomain-containing proteins in transcriptional gene regulation, we focused on possible disruptions to the gametogenesis differentiation programs, postulating that a common theme might emerge. The results indicate a remarkable dichotomy between the sexes in BRWD1's role in gene expression, and thus gamete function.

Microarray analysis of WT and mutant testes revealed that ∼300 genes were misregulated in *Brwd1*$^{-/-}$ mutants. Gene ontology (GO) analysis of the misexpressed genes using DAVID (Huang et al., 2009) showed that the functional clusters to which these genes belonged were, in order: spermatogenesis, cytoskeletal dynamics, flagellum formation, chromatin organization, sperm motility, protein dynamics, and metabolic pathways. About 150 of these genes are differentially expressed in testes (Chalmel et al., 2007), and 88% are clustered as postmeiotic by the GermOnline database (Chalmel et al., 2007; Gattiker et al., 2007). These ontologies and functions are consistent with the *Brwd1* mutant phenotype. Indeed, mouse knockouts of at least 15 of these genes display male sterility or reduced fertility because of defective spermiogenesis. Four of the most dramatically underexpressed genes (∼16–30 fold)—*Tnp2*, *Tssk6*, *Prm2*, and *Tnp1*—are important for the process of chromatin condensation that occurs during spermiogenesis. Mouse mutants of these genes have sperm with abnormal head shapes and defective chromatin condensation, similar to *Brwd1*$^{-/-}$ sperm (Yu et al., 2000; Cho et al., 2001; Zhao et al., 2001; Philipps et al., 2008).

from *Brwd1*$^{-/-}$ oocytes exhibit normal histone deacetylation in spite of the extreme elongation phenotype. The image in C is also shown in Fig. 8 D. (D and E) Immuno-FISH on representative chromosome spreads from WT oocytes indicating the position of centromere–kinetochore domains labeled with CREST antiserum (red). Telomeres were detected after hybridization with a DNA probe (green). (F) Fusion of a distal chromosome fragment (arrow) with the centromeric region of an adjacent univalent chromosome in *Brwd1*$^{-/-}$ oocytes. Note the presence of enlarged telomeric signals. (G) Detection of telomere doublets (arrowhead) in the chromosomes of *Brwd1*$^{-/-}$ oocytes. Bars: (A–C) 10 µm; (D–G) 4 µm.

Mutants of the misexpressed genes *Akap4*, *Calreticulin 3*, *Atp1a4*, *Pldi*, *Gapdhs*, and *Herk4* display impaired sperm motility, as does *Brwd1*$^{-/-}$ sperm (Miki et al., 2004; Huang et al., 2005; Rodriguez and Stewart, 2007; Heinen et al., 2009; Ikawa et al., 2011; Jimenez et al., 2012). Other genes such as *Odf1* and *Oaz3* are important for head–flagellum attachment (Tokuhiro et al., 2009; Yang et al., 2012b). Thus, a severe shortage of the protein products of the misregulated genes is probably responsible for defective spermiogenesis and the resulting infertility in the male *Brwd1*$^{-/-}$ mutants.

The CREM-τ ACT pathway regulates expression of postmeiotic genes important for spermiogenesis (Blendy et al., 1996; Krausz and Sassone-Corsi, 2005; Sassone-Corsi, 2005; Martianov et al., 2010; Kosir et al., 2012). In *Crem* knockout mice, close to 5,000 genes are deregulated in the testes, 2,000 of which have elevated transcripts, and the rest are reduced (Kosir et al., 2012). About 50% of the genes (∼111 genes) that are misregulated in the *Brwd1*$^{-/-}$ mice are also misregulated in the *Crem* knockout. 97 of these genes have been previously clustered as postmeiotic. *Brwd1*, however, is not misregulated in the *Crem* knockout. CREM-τ and BRWD1 may function at least partly independently, considering that 50% of the genes down-regulated in the *Brwd1* are not misregulated in *Crem* mutants. *Crem* knockouts also have a more severe male infertility phenotype, as mutant spermatids arrest before spermiogenesis is complete. This may be attributable to the significantly larger number of misregulated genes in *Crem* mutants.

FLAG-BRWD1 associated with chromatin when expressed in HEK cells. If it functions similarly in round spermatids, it is conceivable that BRWD1, by virtue of its bromodomains, binds acetylated lysine residues of histones found on the nucleosomes of postmeiotic genes, causing transcriptional activation. Indeed, the "protamine domain" comprising the clustered genes *Prm1*, *Prm2*, *Prm3*, and *Tnp2* (all of which are misexpressed in the mutant) progressively gains acetylated histone markers as the germ cells differentiate from spermatocytes to spermatids where they are expressed (Martins and Krawetz, 2007). BRWD1 also has a poly-Q transcriptional activation domain that was reported to activate luciferase expression in vitro (Huang et al., 2003). The WD structures that are present in the BRWD1 protein may also enable it to interact with a wide variety of transcription factors, nucleosome remodelers, and other signaling proteins. Our results suggest that BRWD1 might be part of unique postmeiotic transcriptional-activator complexes that interact with acetylated histones around postmeiotic genes.

BRDT is another testis-specific dual bromodomain-containing protein that is important for postmeiotic transcriptional regulation. An allele lacking the first bromodomain of BRDT (*Brdt*$^{\Delta BD1}$) rendered male, but not female, mice infertile. *Brdt*$^{\Delta BD1/\Delta BD1}$ spermatids failed to elongate properly and had fragmented heterochromatic foci instead of a single chromocenter (Shang et al., 2007; Berkovits and Wolgemuth, 2011). The external appearance and morphologies of the *Brdt*$^{\Delta BD1/\Delta BD1}$ sperm are very similar to that of *Brwd1* mutant sperm. However, far more transcripts were misregulated in the *Brdt*$^{\Delta BD1/\Delta BD1}$ mice (>1,000 genes were up-regulated and >400 down-regulated) than with *Brwd1* mutants. There is also some evidence that BRDT is involved in the 3′ UTR processing of some transcripts (Berkovits et al., 2012). Despite similarities in sperm phenotypes of *Brwd1* and *Brdt* mutants, our data show that BRWD1 is not involved in maintaining or forming the chromocenter or other nuclear domains marked by specific epigenetic marks in round spermatids. BRWD1 might function more locally on specific promoter sequences around postmeiotic genes. It is also possible that other epigenetic markers that were not tested are altered in the mutants. Also, small or local differences of the modifications tested would have been missed by the in situ survey performed here.

In contrast to its role as a positive transcriptional regulator in spermatogenesis, BRWD1 is required for global transcriptional silencing during meiosis onset in oocytes. Nuclear run-on assays revealed that 73.5% of *Brwd1* mutant oocytes failed to properly repress transcriptional activity, even in the presence of an SN configuration. Although this dramatic defect suggested widespread changes in gene expression, this was not the case; the only significantly overexpressed genes were the histone methyl transferase *Mll5*, adipogenesis-associated Mth938 domain containing (*Aamdc*), and Heme oxygenase 1 (*Hmox1*). Although the transcriptomes of WT and *Brwd1* mutant oocytes at the germinal vesicle stage were remarkably similar, further studies are required to determine whether earlier stages of oogenesis, prediplotene, may contain transcriptomic differences that could impact meiotic progression. The disconnect between in situ run-on results and the microarray data led us to explore possible misregulation of repetitive elements, leading to our finding of LINE-1 overexpression. Even though expression was increased only twofold, the sheer number of copies with complete reverse transcription domains (>20,000; Sookdeo et al., 2013) translates into a significant impact in overall transcription.

These results allowed us to generate hypotheses on the mechanistic basis for disrupted epigenetic control of chromosome stability in mutant oocytes. One hypothesis is that *Mll5* misregulation is the key proximal defect. *Mll5* catalyzes trimethylation of histone H3 at lysine 4 (H3K4me3; Sebastian et al., 2009), and its overexpression is known to interfere with cell cycle progression as well as recruitment of the chromosome passenger complex in somatic cells (Sebastian et al., 2009; Liu et al., 2012). Importantly, oocyte-specific deletion of *Mll2*, encoding a histone methyltransferase required for di- and trimethylation of H3K4, was reported to interfere with global transcriptional silencing in preovulatory mouse oocytes (Andreu-Vieyra et al., 2010). Furthermore, IAP but not LINE-1 transposons were also abnormally transcribed in *Mll2* mutant oocytes (Andreu-Vieyra et al., 2010). Overexpression of IAP elements in *Mll2* mutant oocytes and of mouse transposons (MTs) in both *Dicer1*$^{-/-}$ oocytes and mutants of the oocyte-specific Dicer isoform (DicerO) are associated with abnormal meiosis (Murchison et al., 2007; Andreu-Vieyra et al., 2010; Flemr et al., 2013). Meiosis arrest female-1 (MARF1) mutant oocytes, which exhibit a severe meiotic arrest phenotype at the germinal vesicle stage, exhibit LINE-1 overexpression and widespread elevation of double-strand DNA breaks (Su et al., 2012a).

Both transposon expression and repetitive DNA sequences at major satellite transcripts are essential for heterochromatin formation and reprograming of chromatin domains during the

transition from zygote to embryo (Probst and Almouzni, 2011; Casanova et al., 2013). LINE-1 elements are one of the most active types of transposons in the mouse genome, and their expression is regulated by the levels of H3K4me3 at repetitive sequences (Fadloun et al., 2013). Notably, LINE-1 elements have recently been associated with large-scale chromatin remodeling during the process of X chromosome inactivation (Chow et al., 2010; Fadloun et al., 2013). Thus, it is conceivable that changes in epigenetic modifications and large-scale chromatin remodeling brought about by *Mll5* overexpression and LINE-1 elements may account for the chromosome instability phenotype observed in *Brwd1*$^{-/-}$ oocytes.

The type of chromosome segregation defects and lack of proper chromosome condensation in *Brwd1* mutant oocytes is consistent with the presence of major chromosomal structural defects. Yet, markers of pericentric heterochromatin such as ATRX and kinetochore structural proteins detected by the CREST antiserum remain associated with centromeric regions, which suggests predominant damage at distal chromatid regions. Consistent with this notion, our results revealed major telomeric defects in *Brwd1* mutant oocytes. The mechanisms involved in abnormal telomere structure require further investigation. It is possible that BRWD1 association with chromatin, alone or with other proteins, has a key role in chromatin structure independent of a role in transcriptional regulation. Another question concerns whether the persistent double-strand breaks are related to such a hypothetical function or, for example, the persistent LINE-1 expression.

Several pathways are known to be required for chromosome condensation during meiosis. For example, global histone deacetylation during meiosis onset is strictly required for proper chromosome segregation in human and mouse oocytes (De La Fuente, 2006). In addition, histone hyperacetylation induces a striking chromosome elongation phenotype (Yang et al., 2012a). However, chromosomes from *Brwd1* mutant oocytes exhibit normal global histone deacetylation of all the lysine residues evaluated, including H4K16Ac. Monomethylation of histone H4 at lysine 20 is also required for chromosome condensation in mouse oocytes (Oda et al., 2009; Beck et al., 2012). However, the patterns of chromosomal localization of this epigenetic marker are indistinguishable between control and *Brwd1* mutant oocytes. Remarkably, similar to controls, the condensin protein SMC4 was detected at the elongated chromosomes of *Brwd1* mutant oocytes. These results indicate that all the major pathways implicated until now in the control of chromosome condensation are functional in the *Brwd1* mutant oocytes and that BRWD1 may be required for the control of a previously unidentified, yet critical, pathway to regulate chromosome condensation during female meiosis. Further studies will be required to determine whether BRWD1 regulates key factors involved in the onset of global transcriptional repression and proper chromosome condensation during meiosis.

In conclusion, our studies have uncovered distinct and previously unrecognized functions for BRWD1 during oogenesis and spermatogenesis. Bromodomain-containing proteins are usually chromatin-associated and can coordinate the binding of other complexes to chromatin. Bromodomains are also present in a variety of histone acetyl transferases (HATs), some histone methyl transferases (HMTs), and ATP-dependent remodeling enzymes. Genome-wide BRWD1 localization studies, which would be possible with a suitable antibody or epitope-tagged transgene, should illuminate the mechanistic roles of this protein in the epigenetic control of transposon expression and genome integrity in the female germline.

Materials and methods

Mouse strain

Ethylnitrosourea (ENU)-mutagenized mice were generated as described previously (Philipps et al., 2008), and the resulting mutant allele has the designation Brwd1^{repro5} (Mouse Genome Informatics [MGI] ID 3512929). In brief, male C57BL/6J (B6) mice were ENU-mutagenized and bred to C3HeB/FeJ (C3H) females. Pedigrees were backcrossed to C3H mice before further phenotype analysis.

RNA extraction from testis

RNA was prepared from whole testes of WT and mutant mice using TRIzol and purified using RNeasy columns. In brief, the testes from each mouse were homogenized in 700 µl TRIzol, and total RNA was extracted using 140 µl chloroform. The aqueous phase was then separated by centrifugation, and 525 µl of 100% ethanol was added to it. This phase was then directly loaded onto a RNeasy mini column (QIAGEN) and purified according to the manufacturer's instructions.

Microarray analysis (male)

RNA extracted from WT and mutant testes was analyzed for quality using BioAnalyzer (Affymetrix). They were then converted to biotin-labeled complementary RNA (cRNA) fragments according to the protocols described by Affymetrix. Hybridization was performed using Affymetrix MOE430 2.0 gene chips that represent >39,000 uniquely expressed mouse transcripts. Washing and scanning were also done according to Affymetrix protocols. The signals from scanning were analyzed using GCOS software (Affymetrix). The normalized signals were then analyzed using R software using a standard *t* test, and genes were considered up- or down-regulated if they showed a more than twofold difference in expression with a p-value of <0.01. Genes were classified as meiotic, postmeiotic, or somatic using the BioMart mining tool available at the GermOnline database (http://www.germonline.org/index.html). Gene ontology (GO) analysis of the misexpressed genes was performed using DAVID (Huang et al., 2009). We used the MGI database (http://www.informatics.jax.org/) to search for any known knockout phenotypes of genes misregulated in the microarray.

Real-time PCR on testis samples

cDNA was prepared from freshly extracted RNA from WT and mutant testes using Superscript III Reverse transcription according to the manufacturer's instructions. 10 µl of a 1:100 dilution of the above reaction was used as template in a 25-µl master mix using 2× SYBR green. Primers were designed for select genes of the microarray using RealTime PCR Tool (Integrated DNA Technologies) such that the product sizes were 150 bp. Primer sequences are listed in Table S1. Nonspecific amplification was tested for using dissociation curve analysis in the real-time PCR software. Ct values for the different reactions were noted and fold enrichment was calculated as the ratio of $2^{Ctmut}/2^{CtWT}$.

Flow cytometry analysis

A single-cell suspension for flow cytometry analysis was prepared as per the method described by the Fouchet laboratory (Bastos et al., 2005). Seminiferous tubules were dissociated using enzymatic digestion with collagenase Type I for 25 min at 32°C in HBSS (20 mM Hepes, pH 7.2, 1.2 mM $MgSO_4.7H_2O$, 1.3 mM $CaCl_2.2H_2O$, 6.6 mM sodium pyruvate, and 0.05% lactate). This was then filtered through a 40-µm nylon mesh. Tubules were collected from the mesh and incubated again at 32°C for 25 min in HBSS. This was again filtered to remove cell clumps. The cells were then spun down and washed with HBSS. The final pellet was resuspended in HBSS, and the cell count was determined using a hemocytometer. The cells were than fixed in 70% ethanol for 24 h at 4°C. The fixed cells were then washed with 50 µg/ml propidium iodide (PI) and 100 µg/ml RNase in PBS. Cells were then diluted to a final concentration of 1 million cells/ml,

and analysis was performed using a FACSCalibur4 flow cytometer (BD). PI was excited by a 360-nm ultraviolet laser (100 mW), and the emitted red fluorescence was detected with a 630 nm/30 nm band-pass filter. The emitted fluorescence was proportional to DNA content, and three distinct populations were observed in the fluorescence area versus fluorescence width plot. These populations corresponded to "1C," "2C," and "4C" cells in the suspension. The cells in these three distinct populations were counted, and this was plotted in a counts versus fluorescence graph (Fig. 1 C).

Transient transfection of HEK cells

A vector pdream2.1(CMV)FLAGBRWD1 containing the complete BRWD1 sequence with a FLAG tag was purchased from GenScript. FLAGBRWD1 was then amplified from this vector using BIO-X-ACT Long DNA polymerase and cloned into a pCAGGS expression vector (p2453 obtained from Belgian Coordinated Collections of Microorganisms [BCCM]) using the enzyme XhoI. pCAGGS drives expression of full-length FLAGBRWD1 under control of an AG promoter. Clones were verified by sequencing. The pCAGGS-FLAG-BRWD1 plasmid was transfected into HEK cells transiently using TransIT-LT1 reagent from Mirius according to the manufacturer's instructions. In brief, about a million freshly grown HEK cells were plated on a 10-cm plate, 24 h before transfection. 2.5 µg of plasmid DNA was added to 250 µg Opti-MEM I Reduced Serum and mixed gently. 7.5 µl of TransIT-LT1 reagent was added to the DNA mixture and the solution was incubated for 15–30 min at room temperature. The DNA-TransIT-LT1-Opti-MEM mixture was then added on top of the semiconfluent HEK cells. The cells were then grown at 37°C for 72 h to allow for expression of protein. Transfection efficiency was judged by cotransfecting with vector that expressed mCherry protein. Cells expressing mCherry were easily identified as those cells that fluoresced red under a fluorescent microscope.

Immunostaining of transfected cells

HEK cells transiently transfected with pCAGGS-FLAG-BRWD1 were trypsinized, washed, and resuspended in 1% paraformaldehyde for 3 min. After pelleting at 360 *g* for 3 min, the cells were fixed again in 1% PFA for 3 min. 1–10 million cells were then transferred into a chamber-slide and washed three times with PBS. After the final wash, PBS was replaced with blocking solution (2.5% goat serum, 2.5% donkey serum, 1% BSA, 2% gelatin, and 0.1% Triton X-100), and then treated with 0.1% Triton X-100 separately for 1 h for nuclear permeabilization. The blocking solution was then replaced by rabbit anti-FLAG antibody (ab124462; Abcam) at a final concentration of 2 µg/ml and incubated overnight at 4°C. The next day, the cells were washed four times with PBS for 5 min each and then incubated with secondary antibody (Alexa Flour 488 anti–rabbit CY5) at a dilution of 1:80 for 20 min in the dark at room temperature. After washing four times with PBS for 5 min each, the cells were mounted on slides with mounting medium that contained DAPI, which stained for the nuclei. These slides were observed under a fluorescent microscope.

Subcellular fractionation and Western blotting

Transiently transfected HEK cells were harvested and fractionated as per Méndez and Stillman (2000). In brief, ∼10 million cells were harvested, washed thoroughly with PBS, and then suspended in Buffer A (10 mM Hepes, pH 7.9, 10 mM KCl, 1.5 mM $MgCl_2$, 0.34 M sucrose, 10% glycerol, 1 mM DTT, and protease inhibitor cocktail). Triton X-100 was then added to a final concentration of 0.1% and the cell suspension was incubated on ice for 8 min. The suspension was then centrifuged at 1,300 *g* to separate the nuclear fraction (P1) from the cytoplasmic fraction (S1). S1 was further centrifuged at 20,000 *g* at 4°C to collect a clarified supernatant free from debris. P1, however, was washed thoroughly with buffer A and lysed for 30 min using Buffer B (3 mM EDTA, 0.2 mM EGTA, 1 mM DTT, and protease inhibitor cocktail). The lysed fraction was then centrifuged at 1,700 *g* for 5 min at 4°C, separating the supernatant from the pellet. The pellet contained the chromatin, whereas the supernatant contained the nucleoplasmic fraction. The chromatin fraction was further washed once with Buffer B and then resuspended in SDS sample buffer, ready to load in a poly-acrylamide gel.

Protein samples were thus prepared, and 15 µl was loaded onto a 6–15% gradient polyacrylamide gel. After sufficient separation, as judged by the running of a marker in parallel, the gel was dislodged from the electrophoresis apparatus and the proteins were transferred onto a nitrocellulose membrane overnight at 40 V. The next day, the blot was blocked using 15% milk for 1 h and then incubated overnight again with a FLAG antibody at a final concentration of 2 µg/ml (ab124462; Abcam). After a thorough washing with Tween-TBS (five times for 5 min each), the blot was incubated with an anti–rabbit HRP-conjugated secondary antibody that was diluted 1:2,500. The blot was washed again thoroughly with Tween-TBS (five times for 5 min each) and then probed with ECL substrate. An x-ray film was exposed to the blot for 1 min in the dark, developed, and scanned. The blot was then later stripped and reprobed for either fibrillarin (a nuclear marker; ab5821; Abcam) or GAPDH (cytoplasmic marker; ab9485; Abcam) similarly.

Squash preps and immunostaining

Testes were dissected from 2-mo-old adult WT and mutant testes and the albuginea was removed. Seminiferous tubules were eased out and cut into little 10-µm pieces using micro scissors. The tubules were then placed on a Superfrost Plus slide (Thermo Fisher Scientific) and squashed using a glass coverslip, releasing the germ cells onto the slide. The slides were either frozen at −80°C or used directly for immunostaining.

Blocking solution containing 10% goat serum and 0.1% Tween was added directly on top of the cells for 1 h. The slides were then incubated overnight with multiple dilutions of primary antibodies (1:50, 1:250, and 1:500) with a PBS-negative control. They were then washed the next morning three times with PBS for 10 min and then incubated with corresponding secondary at 1:80 for 20 min in the dark. They were washed again three times with PBS and mounted with medium containing DAPI and observed under a fluorescence microscope.

Oocyte collection and culture

Cumulus–oocyte complexes (COCs) were collected from adult female BRWD1 control and mutant mice by follicular aspiration 48 h after intraperitoneal injection with 5 IU pregnant mare serum gonadotropin (PMSG; EMD Millipore) and maintained in MEM medium supplemented with 3 mg/ml bovine serum albumin (MEM/BSA; Sigma-Aldrich), and 10 µM Milrinone (Sigma-Aldrich) to prevent germinal vesicle breakdown (GVBD) at 37°C under an atmosphere of 5% O_2, 5% CO_2, and 90% N_2 (Baumann et al., 2010). Cumulus cells were removed by repeated pipetting and denuded oocytes washed three times in fresh medium before fixation or experimental allocation. For in vitro maturation experiments, denuded oocytes were washed from milrinone and cultured in fresh MEM/BSA supplemented with 5% FBS (HyClone; GE Healthcare) for 14 h under an atmosphere of 5% O_2, 5% CO_2, and 90% N_2 at 37°C before fixation for immunochemistry.

Transcription run-on assays

Transcriptional activity was detected by 5-bromo uridine 5′-triphosphate (Br-UTP; Sigma-Aldrich) incorporation into nascent transcripts as described previously (Aoki et al., 1997; De La Fuente and Eppig, 2001). In brief, detergent-permeabilized oocytes were incubated in transcription buffer (100 mM potassium acetate, 30 mM potassium chloride, 1 mM magnesium chloride, 10 mM sodium phosphate, 2 mM ATP, and 0.4 mM each of GTP, CTP, and Br-UTP) for 20 min at 37°C and fixed overnight in 4% paraformaldehyde in PBS. Incorporated Br-UTP was detected by incubation with 2 µg/ml anti-BrdU (Boehringer Ingelheim) followed by an Alexa Fluor 555–conjugated secondary antibody as described previously (De La Fuente and Eppig, 2001). Labeled oocytes were mounted in antifading medium containing DAPI (Vecta Shield; Vector Laboratories).

Immunochemistry

Whole-mount oocytes were fixed in a 2% paraformaldehyde solution supplemented with 0.1% Triton X-100 for 10 min at room temperature and blocked overnight in 1 mg/ml BSA in PBS, 0.01% Triton X-100. Oocytes were incubated overnight at 4°C with appropriate dilutions of the following antibodies: a mouse anti-BrdU antibody (cross-reactivity with Br-UTP established; 2 µg/ml; Sigma-Aldrich), a rabbit polyclonal anti-histone H4K8ac antibody (1:200; EMD Millipore), a mouse anti-H3K4me3 antibody (1:400; Abcam), a rabbit polyclonal anti-ATRX antibody (1:400; Santa Cruz Biotechnology), and a mouse anti–β-tubulin antibody (1:1,000; Sigma-Aldrich). Surface spread metaphase chromosome figures were prepared as described previously (Baumann et al., 2010). Immunochemistry was conducted by incubation with the following antibodies for 2 h at room temperature: rabbit polyclonal antibodies against histone H4K16ac (1:200; EMD Millipore), H4K20me (1:400; Abcam), H3S10ph (1:1,000; EMD Millipore), H4K5ac (1:200), and Smc4 (1:400) as well as with a human anti–Ana-Centromere C antibody (1:400, Cortex Biochem, Inc.). After several washes in PBS/BSA blocking medium, oocytes were exposed to 1:1,000 dilutions of the appropriate Alexa Fluor 488 or 555 secondary antibodies for 1 h at room temperature followed by DNA counterstaining and mounting in antifading medium.

RNA extraction from oocytes and pathway-focused transcriptional profiling
mRNA was isolated from pools of 100 WT and *Brwd1* mutant oocytes, respectively, using the micro FastTrack 2.0 kit (Invitrogen). 1 µg of mRNA was subjected to DNA elimination and preamplification using RT^2 PreAMP cDNA Synthesis reagents and pathway-specific primers. Actin primers were used as a housekeeping gene control according to the manufacturers' recommendations (SABiosciences; QIAGEN). Expression profiles were established on a Roche LightCycler 480 system using instrument-specific RT^2 SYBR Green qPCR Mastermix reagents (SABiosciences). Raw threshold cycle data were compared using RT^2 Profiler PCR Array Data Analysis software version 3.5 (SABiosciences; QIAGEN) to perform all ΔΔCt-based fold-change calculations. Pairwise comparison (*t* test) between groups of experimental replicates was conducted to define the fold up- or down-regulation and statistical significance thresholds ($P < 0.05$).

Telomere-FISH
Metaphase chromosome spreads obtained from WT and mutant BRDW1 oocytes were subjected to DNA-FISH analysis using an FITC-conjugated telomeric probe (Biosynthesis, Inc.), as described previously (Baumann et al., 2010). In brief, surface spread chromosomes were denatured in 70% formamide (VWR International) in 2× SSC at 85°C for 10 min and subsequently chilled in ice-cold 70% ethanol for 5 min. The telomere probe was denatured for 10 min at 85°C and incubated at 37°C for 1 h. Overnight hybridization was performed in a humidified chamber at room temperature, and stringency washes were conducted in a solution containing 50% formamide in 2× SSC as described previously (De La Fuente et al., 2004).

Image acquisition
Images of spermatogenic cells were acquired using a microscope (BX51; Olympus) equipped with epifluorescence and a UPlan-Apochromat 60×/0.90 NA infinity/0.11–0.23 objective lens. Digital images were captured with a charge-coupled device camera (MagnaFire) using Magnafire 2.0 software (all from Olympus). Images were modified using Photoshop CS6 (Adobe) to minimize background. No gamma correction was applied. Appropriate scales were added to the images.

Immunofluorescence and FISH image acquisition of whole mount and surface spread oocytes was performed at room temperature using Alexa Fluor fluorochromes (Life Technologies) and Vectashield with DAPI (Vector Laboratories) as mounting medium/DNA counterstain. Data analysis was conducted using a DMRE fluorescence microscope (Leica) equipped with an HCX Plan-Apochromat 40×/0.85 NA air objective lens, and with a Plan-Apochromat 63×/1.20 NA water objective lens. Images were captured with a camera (DFC 350F; Leica) using Openlab 3.1.7. software (PerkinElmer), and image processing was performed using Photoshop 2.0 (Adobe) for linear adjustments and cropping of fluorescent images. No gamma adjustments were made.

RNA isolation and quantitative RT-PCR
mRNA was isolated from pools of 35 denuded GV stage oocytes using an miRNeasy kit (QIAGEN) and subsequently subjected to reverse transcription using random hexamer primers and the Superscript III first strand synthesis system (Invitrogen). The resulting cDNA was used for quantitative expression analysis of major satellite repeat transcripts as well as transposons by real-time PCR using 2× Brilliant II real-time PCR reagents (Agilent Technologies) on an MX3005p apparatus (Agilent Technologies) using the following primer sequences: IAP-fwd, 5′-ACAAGAAAAGAAGCCCGTGA-3′; IAP-rev, 5′-GCCAGAACATGTGTCAATGG-3′; Line1-fwd, 5′-GAGACATAACAACAGATCCTGA-3′; Line1-rev, 5′-AACTTTGGTACCTGGTATCTG-3′; Mt-fwd, 5′-TGTTAAGAGCTCTGTCGGATGTTG-3′; Mt-rev, 5′-ACTGATTCTTCAGTCCCAGCTAAC-3′; Rpl19-fwd, 5′-CCGCTGCGGGAAAAAGAAG-3′; Rpl19-rev, 5′-CAGCCCATCCTTGATCAGCTT-3′; Sineb1-fwd, 5′-GTGGCGCACGCCTTTAATC-3′; Sineb1-rev, 5′-GACAGGGTTTCTCTGTGTAG-3′; Sineb2-fwd, 5′-GAGATGGCTCAGTGGTTAAG-3′; and Sineb2-rev, 5′-CTGTCTTCAGACACTCCAG-3′ (Su et al., 2012a). Major satellite-fwd, 5′-GATTTCGTCATTTTTCAAGTCGTC-3′; Major satellite-rev, 5′-GCACACTGAAGGACCTGGAATATG-3′.

Microarray analysis from GV-stage oocytes
Oocyte collection, RNA extraction, and amplification for microarray analysis was conducted as described previously (Su et al., 2012a). In brief, total RNA was extracted from 100 oocytes per sample and genotype using the PicoPure RNA isolation kit (Life Technologies) according to the manufacturer's instructions. Before cDNA synthesis and amplification using the Nugen Ovation Pico WTA System (NuGEN Technologies, Inc.), quality and quantity of the RNA were analyzed with a Bioanalyzer 2100 (Agilent Technologies), the RNA 6000 Pico LabChip assay (Agilent Technologies), and the Quant-iT RiboGreen Reagent according to supplier's instructions (Life Technologies). cDNA was then fragmented and biotin-labeled using Encore Biotin Module (NuGEN Technologies, Inc.) before hybridization to Affymetrix GeneChip mouse Gene 1.0 ST arrays (Affymetrix). Posthybridization staining and washing were performed using the Fluidics Station 450 instrument (Affymetrix) according to manufacturer's instructions followed by scanning of the arrays with a GeneChip 3000 laser confocal slide scanner (Affymetrix) and quantification using Gene Chip Operating Software version 1.2 (GCOS; Affymetrix). Average signal intensities per probe set within arrays were calculated by the Expression Console (Version 1.1) software (Affymetrix) using the RMA method, which includes convolution background correction. Summarization was based on a multiarray model fit robustly using the median polish algorithm, and sketch-quantile normalization. We used a standard approach for data normalization of each probe set. We log2-transformed the raw intensities for all probes, and log2-transformed data were used to minimize outlier's impact and for quantile normalization. This method normalizes data based on the magnitude of probe set intensities and brings the data from different microarrays onto a common scale.

We used scatter plots of log2-transformed, quantile-normalized intensities to compare the degree of similarity (correlation) of samples within a group to the degree of similarities of samples between groups yielding r values of $r = 0.9944$ and $r = 0.9943$ between the first and second biological replicates, confirming that the microarray results on each biological replicate were highly reproducible.

Statistical analysis
Data are presented as the mean percentage of at least three independent experiments; variation among replicates is presented as the standard deviation. Data were analyzed using the Student's *t* test and differences were considered significant when $P < 0.05$.

Online supplemental material
Fig. S1 shows additional information displayed in Fig. 9 indicating the presence of normal histone methylation at lysine 20 (H4K20me1) in *Brwd1*$^{-/-}$ oocytes. Fig. S2 shows the patterns of condensing protein (SMC4) localization in the chromosomes of WT and *Brwd1*$^{-/-}$ oocytes. Table S1 provides a list of primer sequences used for real-time PCR. Tables S2 and S3 provide a list of annotated genes with at least twofold lower expression (S2) or higher expression (S3) in *Brwd1*$^{-/-}$ oocytes compared with WT oocytes. Online supplemental material is available at http://www.jcb.org/cgi/content/full/jcb.201404109/DC1.

We thank the service core at The Jackson Laboratory for assistance with microarrays.

This work was supported by National Institutes of Health (NIH) grant P01 HD42137 to J.J. Eppig and J.C. Schimenti, and by NIH 2RO1-HD042740 grant and the Georgia Cancer Coalition to R. De La Fuente.

The authors declare no competing financial interests.

Submitted: 21 April 2014
Accepted: 25 November 2014

References

Abe, K., A. Inoue, M.G. Suzuki, and F. Aoki. 2010. Global gene silencing is caused by the dissociation of RNA polymerase II from DNA in mouse oocytes. *J. Reprod. Dev.* 56:502–507. http://dx.doi.org/10.1262/jrd.10-068A

Akiyama, T., M. Nagata, and F. Aoki. 2006. Inadequate histone deacetylation during oocyte meiosis causes aneuploidy and embryo death in mice. *Proc. Natl. Acad. Sci. USA*. 103:7339–7344. http://dx.doi.org/10.1073/pnas.0510946103

Andreu-Vieyra, C.V., R. Chen, J.E. Agno, S. Glaser, K. Anastassiadis, A.F. Stewart, and M.M. Matzuk. 2010. MLL2 is required in oocytes for bulk histone 3 lysine 4 trimethylation and transcriptional silencing. *PLoS Biol.* 8:e1000453. http://dx.doi.org/10.1371/journal.pbio.1000453

Aoki, F., D.M. Worrad, and R.M. Schultz. 1997. Regulation of transcriptional activity during the first and second cell cycles in the preimplantation mouse embryo. *Dev. Biol.* 181:296–307. http://dx.doi.org/10.1006/dbio.1996.8466

Bastos, H., B. Lassalle, A. Chicheportiche, L. Riou, J. Testart, I. Allemand, and P. Fouchet. 2005. Flow cytometric characterization of viable meiotic and postmeiotic cells by Hoechst 33342 in mouse spermatogenesis. *Cytometry A*. 65A:40–49. http://dx.doi.org/10.1002/cyto.a.20129

Baumann, C., M.M. Viveiros, and R. De La Fuente. 2010. Loss of maternal ATRX results in centromere instability and aneuploidy in the mammalian

oocyte and pre-implantation embryo. *PLoS Genet.* 6:e1001137. http://dx.doi.org/10.1371/journal.pgen.1001137

Beck, D.B., H. Oda, S.S. Shen, and D. Reinberg. 2012. PR-Set7 and H4K20me1: at the crossroads of genome integrity, cell cycle, chromosome condensation, and transcription. *Genes Dev.* 26:325–337. http://dx.doi.org/10.1101/gad.177444.111

Berkovits, B.D., and D.J. Wolgemuth. 2011. The first bromodomain of the testis-specific double bromodomain protein Brdt is required for chromocenter organization that is modulated by genetic background. *Dev. Biol.* 360:358–368. http://dx.doi.org/10.1016/j.ydbio.2011.10.005

Berkovits, B.D., and D.J. Wolgemuth. 2013. The role of the double bromodomain-containing BET genes during mammalian spermatogenesis. *Curr. Top. Dev. Biol.* 102:293–326. http://dx.doi.org/10.1016/B978-0-12-416024-8.00011-8

Berkovits, B.D., L. Wang, P. Guarnieri, and D.J. Wolgemuth. 2012. The testis-specific double bromodomain-containing protein BRDT forms a complex with multiple spliceosome components and is required for mRNA splicing and 3′-UTR truncation in round spermatids. *Nucleic Acids Res.* 40:7162–7175. http://dx.doi.org/10.1093/nar/gks342

Blendy, J.A., K.H. Kaestner, G.F. Weinbauer, E. Nieschlag, and G. Schütz. 1996. Severe impairment of spermatogenesis in mice lacking the CREM gene. *Nature*. 380:162–165. http://dx.doi.org/10.1038/380162a0

Bottomley, M.J. 2004. Structures of protein domains that create or recognize histone modifications. *EMBO Rep.* 5:464–469. http://dx.doi.org/10.1038/sj.embor.7400146

Casanova, M., M. Pasternak, F. El Marjou, P. Le Baccon, A.V. Probst, and G. Almouzni. 2013. Heterochromatin reorganization during early mouse development requires a single-stranded noncoding transcript. *Cell Reports*. 4:1156–1167. http://dx.doi.org/10.1016/j.celrep.2013.08.015

Chalmel, F., A.D. Rolland, C. Niederhauser-Wiederkehr, S.S. Chung, P. Demougin, A. Gattiker, J. Moore, J.J. Patard, D.J. Wolgemuth, B. Jégou, and M. Primig. 2007. The conserved transcriptome in human and rodent male gametogenesis. *Proc. Natl. Acad. Sci. USA*. 104:8346–8351. http://dx.doi.org/10.1073/pnas.0701883104

Cho, C., W.D. Willis, E.H. Goulding, H. Jung-Ha, Y.C. Choi, N.B. Hecht, and E.M. Eddy. 2001. Haploinsufficiency of protamine-1 or -2 causes infertility in mice. *Nat. Genet.* 28:82–86. http://dx.doi.org/10.1038/ng0501-82

Chow, J.C., C. Ciaudo, M.J. Fazzari, N. Mise, N. Servant, J.L. Glass, M. Attreed, P. Avner, A. Wutz, E. Barillot, et al. 2010. LINE-1 activity in facultative heterochromatin formation during X chromosome inactivation. *Cell*. 141:956–969. http://dx.doi.org/10.1016/j.cell.2010.04.042

De La Fuente, R. 2006. Chromatin modifications in the germinal vesicle (GV) of mammalian oocytes. *Dev. Biol.* 292:1–12. http://dx.doi.org/10.1016/j.ydbio.2006.01.008

De La Fuente, R., and J.J. Eppig. 2001. Transcriptional activity of the mouse oocyte genome: companion granulosa cells modulate transcription and chromatin remodeling. *Dev. Biol.* 229:224–236. http://dx.doi.org/10.1006/dbio.2000.9947

De La Fuente, R., M.M. Viveiros, K.H. Burns, E.Y. Adashi, M.M. Matzuk, and J.J. Eppig. 2004. Major chromatin remodeling in the germinal vesicle (GV) of mammalian oocytes is dispensable for global transcriptional silencing but required for centromeric heterochromatin function. *Dev. Biol.* 275:447–458. http://dx.doi.org/10.1016/j.ydbio.2004.08.028

De La Fuente, R., C. Baumann, T. Fan, A. Schmidtmann, I. Dobrinski, and K. Muegge. 2006. Lsh is required for meiotic chromosome synapsis and retrotransposon silencing in female germ cells. *Nat. Cell Biol.* 8:1448–1454. http://dx.doi.org/10.1038/ncb1513

Fadloun, A., S. Le Gras, B. Jost, C. Ziegler-Birling, H. Takahashi, E. Gorab, P. Carninci, and M.E. Torres-Padilla. 2013. Chromatin signatures and retrotransposon profiling in mouse embryos reveal regulation of LINE-1 by RNA. *Nat. Struct. Mol. Biol.* 20:332–338. http://dx.doi.org/10.1038/nsmb.2495

Flemr, M., R. Malik, V. Franke, J. Nejepinska, R. Sedlacek, K. Vlahovicek, and P. Svoboda. 2013. A retrotransposon-driven dicer isoform directs endogenous small interfering RNA production in mouse oocytes. *Cell*. 155:807–816. http://dx.doi.org/10.1016/j.cell.2013.10.001

Foulkes, N.S., B. Mellström, E. Benusiglio, and P. Sassone-Corsi. 1992. Developmental switch of CREM function during spermatogenesis: from antagonist to activator. *Nature*. 355:80–84. http://dx.doi.org/10.1038/355080a0

Gattiker, A., C. Niederhauser-Wiederkehr, J. Moore, L. Hermida, and M. Primig. 2007. The GermOnline cross-species systems browser provides comprehensive information on genes and gene products relevant for sexual reproduction. *Nucleic Acids Res.* 35:D457–D462. http://dx.doi.org/10.1093/nar/gkl957

Heinen, T.J., F. Staubach, D. Häming, and D. Tautz. 2009. Emergence of a new gene from an intergenic region. *Curr. Biol.* 19:1527–1531. http://dx.doi.org/10.1016/j.cub.2009.07.049

Hoyer-Fender, S., P.B. Singh, and D. Motzkus. 2000. The murine heterochromatin protein M31 is associated with the chromocenter in round spermatids and is a component of mature spermatozoa. *Exp. Cell Res.* 254:72–79. http://dx.doi.org/10.1006/excr.1999.4729

Huang, H., I. Rambaldi, E. Daniels, and M. Featherstone. 2003. Expression of the Wdr9 gene and protein products during mouse development. *Dev. Dyn.* 227:608–614. http://dx.doi.org/10.1002/dvdy.10344

Huang, Z., P.R. Somanath, R. Chakrabarti, E.M. Eddy, and S. Vijayaraghavan. 2005. Changes in intracellular distribution and activity of protein phosphatase PP1γ2 and its regulating proteins in spermatozoa lacking AKAP4. *Biol. Reprod.* 72:384–392. http://dx.doi.org/10.1095/biolreprod.104.034140

Huang, W., B.T. Sherman, and R.A. Lempicki. 2009. Systematic and integrative analysis of large gene lists using DAVID bioinformatics resources. *Nat. Protoc.* 4:44–57. http://dx.doi.org/10.1038/nprot.2008.211

Hudson, B.P., M.A. Martinez-Yamout, H.J. Dyson, and P.E. Wright. 2000. Solution structure and acetyl-lysine binding activity of the GCN5 bromodomain. *J. Mol. Biol.* 304:355–370. http://dx.doi.org/10.1006/jmbi.2000.4207

Ikawa, M., K. Tokuhiro, R. Yamaguchi, A.M. Benham, T. Tamura, I. Wada, Y. Satouh, N. Inoue, and M. Okabe. 2011. Calsperin is a testis-specific chaperone required for sperm fertility. *J. Biol. Chem.* 286:5639–5646. http://dx.doi.org/10.1074/jbc.M110.140152

Jimenez, T., G. Sánchez, and G. Blanco. 2012. Activity of the Na,K-ATPase α4 isoform is regulated during sperm capacitation to support sperm motility. *J. Androl.* 33:1047–1057. http://dx.doi.org/10.2164/jandrol.111.015545

Kim, S., S.H. Namekawa, L.M. Niswander, J.O. Ward, J.T. Lee, V.J. Bardwell, and D. Zarkower. 2007. A mammal-specific Doublesex homolog associates with male sex chromatin and is required for male meiosis. *PLoS Genet.* 3:e62. http://dx.doi.org/10.1371/journal.pgen.0030062

Kosir, R., P. Juvan, M. Perse, T. Budefeld, G. Majdic, M. Fink, P. Sassone-Corsi, and D. Rozman. 2012. Novel insights into the downstream pathways and targets controlled by transcription factors CREM in the testis. *PLoS ONE*. 7:e31798. http://dx.doi.org/10.1371/journal.pone.0031798

Kotaja, N., D. De Cesare, B. Macho, L. Monaco, S. Brancorsini, E. Goossens, H. Tournaye, A. Gansmuller, and P. Sassone-Corsi. 2004. Abnormal sperm in mice with targeted deletion of the act (activator of cAMP-responsive element modulator in testis) gene. *Proc. Natl. Acad. Sci. USA*. 101:10620–10625. http://dx.doi.org/10.1073/pnas.0401947101

Krausz, C., and P. Sassone-Corsi. 2005. Genetic control of spermiogenesis: insights from the CREM gene and implications for human infertility. *Reprod. Biomed. Online*. 10:64–71. http://dx.doi.org/10.1016/S1472-6483(10)60805-X

Lee, J., S. Ogushi, M. Saitou, and T. Hirano. 2011. Condensins I and II are essential for construction of bivalent chromosomes in mouse oocytes. *Mol. Biol. Cell*. 22:3465–3477. http://dx.doi.org/10.1091/mbc.E11-05-0423

Liu, J., F. Cheng, and L.-W. Deng. 2012. MLL5 maintains genomic integrity by regulating the stability of the chromosomal passenger complex through a functional interaction with Borealin. *J. Cell Sci.* 125:4676–4685. http://dx.doi.org/10.1242/jcs.110411

Liu, Z., S. Zhou, L. Liao, X. Chen, M. Meistrich, and J. Xu. 2010. Jmjd1a demethylase-regulated histone modification is essential for cAMP-response element modulator-regulated gene expression and spermatogenesis. *J. Biol. Chem.* 285:2758–2770. http://dx.doi.org/10.1074/jbc.M109.066845

Martianov, I., G.M. Fimia, A. Dierich, M. Parvinen, P. Sassone-Corsi, and I. Davidson. 2001. Late arrest of spermiogenesis and germ cell apoptosis in mice lacking the TBP-like *TLF/TRF2* gene. *Mol. Cell*. 7:509–515. http://dx.doi.org/10.1016/S1097-2765(01)00198-8

Martianov, I., S. Brancorsini, A. Gansmuller, M. Parvinen, I. Davidson, and P. Sassone-Corsi. 2002. Distinct functions of TBP and TLF/TRF2 during spermatogenesis: requirement of TLF for heterochromatic chromocenter formation in haploid round spermatids. *Development*. 129:945–955.

Martianov, I., M.A. Choukrallah, A. Krebs, T. Ye, S. Legras, E. Rijkers, W. Van Ijcken, B. Jost, P. Sassone-Corsi, and I. Davidson. 2010. Cell-specific occupancy of an extended repertoire of CREM and CREB binding loci in male germ cells. *BMC Genomics*. 11:530. http://dx.doi.org/10.1186/1471-2164-11-530

Martins, R.P., and S.A. Krawetz. 2007. Decondensing the protamine domain for transcription. *Proc. Natl. Acad. Sci. USA*. 104:8340–8345. http://dx.doi.org/10.1073/pnas.0700076104

Matzuk, M.M., and D.J. Lamb. 2008. The biology of infertility: research advances and clinical challenges. *Nat. Med.* 14:1197–1213. http://dx.doi.org/10.1038/nm.f.1895

Méndez, J., and B. Stillman. 2000. Chromatin association of human origin recognition complex, cdc6, and minichromosome maintenance proteins during the cell cycle: assembly of prereplication complexes in late mitosis. *Mol. Cell. Biol.* 20:8602–8612. http://dx.doi.org/10.1128/MCB.20.22.8602-8612.2000

Miki, K., W. Qu, E.H. Goulding, W.D. Willis, D.O. Bunch, L.F. Strader, S.D. Perreault, E.M. Eddy, and D.A. O'Brien. 2004. Glyceraldehyde 3-phosphate dehydrogenase-S, a sperm-specific glycolytic enzyme, is required for sperm motility and male fertility. *Proc. Natl. Acad. Sci. USA*. 101:16501–16506. http://dx.doi.org/10.1073/pnas.0407708101

Mora-Bermúdez, F., D. Gerlich, and J. Ellenberg. 2007. Maximal chromosome compaction occurs by axial shortening in anaphase and depends on Aurora kinase. *Nat. Cell Biol.* 9:822–831. http://dx.doi.org/10.1038/ncb1606

Murchison, E.P., P. Stein, Z. Xuan, H. Pan, M.Q. Zhang, R.M. Schultz, and G.J. Hannon. 2007. Critical roles for Dicer in the female germline. *Genes Dev.* 21:682–693. http://dx.doi.org/10.1101/gad.1521307

Nantel, F., L. Monaco, N.S. Foulkes, D. Masquilier, M. LeMeur, K. Henriksén, A. Dierich, M. Parvinen, and P. Sassone-Corsi. 1996. Spermiogenesis deficiency and germ-cell apoptosis in CREM-mutant mice. *Nature*. 380:159–162. http://dx.doi.org/10.1038/380159a0

Oda, H., I. Okamoto, N. Murphy, J. Chu, S.M. Price, M.M. Shen, M.E. Torres-Padilla, E. Heard, and D. Reinberg. 2009. Monomethylation of histone H4-lysine 20 is involved in chromosome structure and stability and is essential for mouse development. *Mol. Cell. Biol.* 29:2278–2295. http://dx.doi.org/10.1128/MCB.01768-08

Okada, Y., G. Scott, M.K. Ray, Y. Mishina, and Y. Zhang. 2007. Histone demethylase JHDM2A is critical for Tnp1 and Prm1 transcription and spermatogenesis. *Nature*. 450:119–123. http://dx.doi.org/10.1038/nature06236

Philipps, D.L., K. Wigglesworth, S.A. Hartford, F. Sun, S. Pattabiraman, K. Schimenti, M. Handel, J.J. Eppig, and J.C. Schimenti. 2008. The dual bromodomain and WD repeat-containing mouse protein BRWD1 is required for normal spermiogenesis and the oocyte-embryo transition. *Dev. Biol.* 317:72–82. http://dx.doi.org/10.1016/j.ydbio.2008.02.018

Probst, A.V., and G. Almouzni. 2011. Heterochromatin establishment in the context of genome-wide epigenetic reprogramming. *Trends Genet.* 27:177–185. http://dx.doi.org/10.1016/j.tig.2011.02.002

Probst, A.V., I. Okamoto, M. Casanova, F. El Marjou, P. Le Baccon, and G. Almouzni. 2010. A strand-specific burst in transcription of pericentric satellites is required for chromocenter formation and early mouse development. *Dev. Cell*. 19:625–638. http://dx.doi.org/10.1016/j.devcel.2010.09.002

Rodriguez, C.I., and C.L. Stewart. 2007. Disruption of the ubiquitin ligase HERC4 causes defects in spermatozoon maturation and impaired fertility. *Dev. Biol.* 312:501–508. http://dx.doi.org/10.1016/j.ydbio.2007.09.053

Sasaki, H., and Y. Matsui. 2008. Epigenetic events in mammalian germ-cell development: reprogramming and beyond. *Nat. Rev. Genet.* 9:129–140. http://dx.doi.org/10.1038/nrg2295

Sassone-Corsi, P. 2002. Unique chromatin remodeling and transcriptional regulation in spermatogenesis. *Science*. 296:2176–2178. http://dx.doi.org/10.1126/science.1070963

Sassone-Corsi, P. 2005. Transcription factors governing male fertility. *Andrologia.* 37:228–229. http://dx.doi.org/10.1111/j.1439-0272.2005.00701.x

Sebastian, S., P. Sreenivas, R. Sambasivan, S. Cheedipudi, P. Kandalla, G.K. Pavlath, and J. Dhawan. 2009. MLL5, a trithorax homolog, indirectly regulates H3K4 methylation, represses cyclin A2 expression, and promotes myogenic differentiation. *Proc. Natl. Acad. Sci. USA*. 106:4719–4724. http://dx.doi.org/10.1073/pnas.0807136106

Shang, E., H.D. Nickerson, D. Wen, X. Wang, and D.J. Wolgemuth. 2007. The first bromodomain of Brdt, a testis-specific member of the BET sub-family of double-bromodomain-containing proteins, is essential for male germ cell differentiation. *Development*. 134:3507–3515. http://dx.doi.org/10.1242/dev.004481

Shintomi, K., and T. Hirano. 2011. The relative ratio of condensin I to II determines chromosome shapes. *Genes Dev.* 25:1464–1469. http://dx.doi.org/10.1101/gad.2060311

Sookdeo, A., C.M. Hepp, M.A. McClure, and S. Boissinot. 2013. Revisiting the evolution of mouse LINE-1 in the genomic era. *Mob. DNA*. 4:3. http://dx.doi.org/10.1186/1759-8753-4-3

Su, Y.-Q., K. Sugiura, F. Sun, J.K. Pendola, G.A. Cox, M.A. Handel, J.C. Schimenti, and J.J. Eppig. 2012a. MARF1 regulates essential oogenic processes in mice. *Science*. 335:1496–1499. http://dx.doi.org/10.1126/science.1214680

Su, Y.-Q., F. Sun, M.A. Handel, J.C. Schimenti, and J.J. Eppig. 2012b. Meiosis arrest female 1 (MARF1) has nuage-like function in mammalian oocytes. *Proc. Natl. Acad. Sci. USA*. 109:18653–18660. http://dx.doi.org/10.1073/pnas.1216904109

Tokuhiro, K., A. Isotani, S. Yokota, Y. Yano, S. Oshio, M. Hirose, M. Wada, K. Fujita, Y. Ogawa, M. Okabe, et al. 2009. OAZ-t/OAZ3 is essential for rigid connection of sperm tails to heads in mouse. *PLoS Genet.* 5:e1000712. http://dx.doi.org/10.1371/journal.pgen.1000712

Weinbauer, G.F., R. Behr, M. Bergmann, and E. Nieschlag. 1998. Testicular cAMP responsive element modulator (CREM) protein is expressed in round spermatids but is absent or reduced in men with round spermatid maturation arrest. *Mol. Hum. Reprod.* 4:9–15. http://dx.doi.org/10.1093/molehr/4.1.9

Yang, F., C. Baumann, M.M. Viveiros, and R. De La Fuente. 2012a. Histone hyperacetylation during meiosis interferes with large-scale chromatin remodeling, axial chromatid condensation and sister chromatid separation in the mammalian oocyte. *Int. J. Dev. Biol.* 56:889–899. http://dx.doi.org/10.1387/ijdb.120246rd

Yang, K., A. Meinhardt, B. Zhang, P. Grzmil, I.M. Adham, and S. Hoyer-Fender. 2012b. The small heat shock protein ODF1/HSPB10 is essential for tight linkage of sperm head to tail and male fertility in mice. *Mol. Cell. Biol.* 32:216–225. http://dx.doi.org/10.1128/MCB.06158-11

Yu, Y.E., Y. Zhang, E. Unni, C.R. Shirley, J.M. Deng, L.D. Russell, M.M. Weil, R.R. Behringer, and M.L. Meistrich. 2000. Abnormal spermatogenesis and reduced fertility in transition nuclear protein 1-deficient mice. *Proc. Natl. Acad. Sci. USA*. 97:4683–4688. http://dx.doi.org/10.1073/pnas.97.9.4683

Zeng, L., and M.M. Zhou. 2002. Bromodomain: an acetyl-lysine binding domain. *FEBS Lett.* 513:124–128. http://dx.doi.org/10.1016/S0014-5793(01)03309-9

Zhang, D., T.L. Penttila, P.L. Morris, M. Teichmann, and R.G. Roeder. 2001. Spermiogenesis deficiency in mice lacking the Trf2 gene. *Science*. 292:1153–1155. http://dx.doi.org/10.1126/science.1059188

Zhao, M., C.R. Shirley, Y.E. Yu, B. Mohapatra, Y. Zhang, E. Unni, J.M. Deng, N.A. Arango, N.H. Terry, M.M. Weil, et al. 2001. Targeted disruption of the transition protein 2 gene affects sperm chromatin structure and reduces fertility in mice. *Mol. Cell. Biol.* 21:7243–7255. http://dx.doi.org/10.1128/MCB.21.21.7243-7255.2001